The Thesis committee for Muneeb Ahmad

Certifies that this is the approved version of the following thesis:

Rate of Penetration (ROP) Enhancement in Shales through Osmotic Processes

APPROVED BY

SUPERVISING COMMITTEE:

Supervisor: _____

Eric van Oort

_____

Carlos Torres-Verdin

Rate of Penetration (ROP) Enhancement in Shales through Osmotic Processes

by

Muneeb Ahmad, B.E.

Thesis

Presented to the Faculty of the Graduate School of

The University of Texas at Austin

in Partial Fulfillment

of the Requirements

for the Degree of

Master of Science in Engineering

The University of Texas at Austin

May 2015

Dedication

To my parents.

Acknowledgements

I would like to praise and thank ALLAH, the Almighty, without whose permission I could not have finished this research. I express my sincere gratitude to my advisor Dr. Eric van Oort for offering me an opportunity to work in his research team. His constant guidance and encouragement within all aspects of this research is a major reason for its success. I am also grateful to Dr. Carlos Torres-Verdin for being a co-reader of my thesis and for providing valuable advice and feedback.

I would like to thank Baker Hughes for their financial and technical support for this project. Within Baker Hughes, I would like to particularly thank Reed Spencer, Aaron Dick, Paul Lutes, Wesley Moore, Suresh Patel, Dennis Clapper, Barrett Scrivner, Paige Kiesewetter, and Roy Ledgerwood for all their help, support and input. I would also like to thank Cabot Specialty Drilling Fluids, and in particular Siv Howard, for their generous support in providing the formate fluids used in this study.

I am also grateful to all the colleagues in our research group especially Bez Hoxha and Ali Karimi for their support and assistance in conducting the experimental work.

Sincere thanks to Tesse Smitherman, Frankie Hart, Glen Baum, and Gary Miscoe for their technical and administrative support.

Last but not least, I owe my deepest gratitude to my family for always believing in me and supporting my decisions. Their unconditional love, encouragement, and sacrifice are my main source of inspiration.

Abstract

Rate of Penetration (ROP) Enhancement in Shales through Osmotic Processes

Muneeb Ahmad, M.S.E.

The University of Texas at Austin, 2015

Supervisor: Eric van Oort

Shales and other clay-bearing rocks make up 70% to 80% of all formations drilled globally. In addition, according to the US Energy Information Administration, as of June 2013, approximately 26% of the technically recoverable hydrocarbon resources of the United States were in the form of shale tight oil and shale gas. Accordingly, there has been an increasing focus on efficient drilling of deep and tight shale formations. However, serious drilling problems such as bit balling and wellbore instability are encountered while drilling shale, especially in deep, high-pressure wells. Most of these drilling problems are not caused by the mechanical strength of the rock but by the chemically reactive nature of such formations, causing rock cuttings to stick to the bit. Such an undesirable effect decreases the rate of penetration (ROP) and has a damaging effect on the wellbore. Previous approaches to this problem were based on either improving the drilling hydraulics or the polycrystalline diamond compact (PDC) bit design, or modifying the mud chemistry.

This thesis introduces a new approach to prevent adherence of shale cuttings to the bit by taking advantage of the phenomenon of chemical osmosis. Chemical osmosis occurs when fluid movement is governed by chemical potential gradients. Drilling with a high salinity/ low water activity drilling mud gives inception to movement of water out of shale cuttings toward the drilling bit due to the difference of water activity between the shale and the drilling fluid. While previous studies showed that the movement of water out of shales also helps to mechanically stabilize them, this study suggests that such a dehydration of formation rock cuttings also prevents shale cuttings from sticking to the bit, resulting in higher rates of penetration. It is also suggested that the same mechanism is responsible for achieving the ROP benefits from high salinity formate muds, which enabled three times faster drilling than the oil-based mud at high densities during the deep trek testing in 2002.

Support for the proposed mechanism is provided by an extensive set of laboratory measurements, ranging from simple hot-rolling tests that measure accretion tendencies of shale on steel to realistic drilling tests on full-scale equipment and actual PDC bits under downhole conditions. Results from the drilling tests indicate that both low and high salinity formate muds outperform the corresponding weight water-based muds in the Mancos shale, by yielding 50% to 60% higher ROP especially at a higher weight on bit (WOB; i.e., corresponding to greater depths). Results from field trials with formate muds for ROP enhancement in Canada indicate significantly enhanced drilling rates with respect to those of oil/synthetic mud causing an approximately 50% reduction in average drilling time, thereby supporting the merits of chemical osmosis for ROP enhancement.

Table of Contents

List of Tables

List of Figures

Chapter 1: Research/Thesis Overview

1.1 INTRODUCTION

Over the past few years, tight oil and shale gas resources have completely transformed the US oil and gas market. According to the US Energy Information Administration (EIA), tight oil's contribution to the total US crude oil production increased from 12% to 35% between 2008 and 2012. In its Annual Energy Outlook of 2014, the EIA estimated this contribution to further increase to 50% by the end of 2019. In the same report, the EIA conservatively estimated that 26% of the recoverable oil and gas resources of the United States alone are contained in shale formations (U.S. Energy Information Administration, 2014). Accordingly, there has been an increasing focus on efficient drilling of deep and tight shale formations. However, serious drilling problems are associated with shale drilling, especially in deep and high-pressure wells. Common examples are bit balling, wellbore instability and low penetration rates, all resulting in high drilling costs. Drilling with PDC bits in oil- or synthetic-based muds is the best possible combination adopted by drillers across the world to address these problems. However, tightening environmental regulations and high costs associated with using oil-based muds are some of the reasons why operators are investigating ways to deal with these problems and would still consider switching to water-based mud systems if they would present viable alternatives.

1.2 RESEARCH OBJECTIVE

In 2002, the Deep Trek program tested different drill bits and advanced drilling fluids under high-pressure conditions. The objective was to devise an economical and efficient mud system that can drill deep oil and gas formations. Results from the study indicate that 16ppg cesium formate mud out-drilled 16ppg oil-based mud (OBM) by a large margin. At higher weight on bit (WOB) (e.g., at 20,000 lbs.), formate mud recorded twice as much rate of penetration (ROP) as 16ppg OBM. Higher hydraulic horsepower per square inch (HSI) in the presence of formate mud as compared to that in OBM (5 vs. 2) was undoubtedly one factor that contributed to this increase in ROP. Moreover, the Deep Trek team attributed this improvement in ROP to the increase in bit aggressiveness and efficiency caused by the presence of clear/low solids cesium formate mud. They related this efficiency to an improvement in minimum specific energy (MSE); however, they provided no insight into the mechanism/principle behind this effect. Similarly, the better performance of cesium formate mud even in the presence of 40ppb solids was not duly explained.

The hypothesis of this investigation is that together with better bit hydraulics and higher bit aggressiveness and efficiency, another mechanism is causing higher ROPs in cesium formate mud even in the presence of simulated solids. It is argued that this mechanism is chemical osmosis, which works similarly to electro-osmosis to draw water from the drilled cuttings out toward the drill bit, lubricate the drill bit and minimize the sticking tendency of the rock cuttings. All these effects contribute to better bit cleaning, and ultimately results in enhanced ROP.

The basic objective of this research was to study the effect of chemical osmosis on bit balling reduction and to determine how this reduction enhances the ROP in an actual drilling environment. Experimental investigation of the proposed study included large-scale drilling tests similar to those performed during the Deep Trek experiments, but with a consistent HSI so as to eliminate any preferential influence of hydraulics. Laboratory-scaled accretion tests were also carried out to study the osmotic effect on bit balling reduction.

1.3 THESIS OUTLINE

Chapter 2 starts with a brief introduction of bit balling problem and its various mitigation techniques, including electro-osmosis experiments and their results. Subsequently, the mechanism of the chemical osmosis process and its various applications in the drilling fluids industry is discussed. A separate section explains the Deep Trek experiments and results. The chapter concludes with a brief literature review of formate fluids.

Chapter 3 contains the experimental section, which explains the testing procedures and setups. The first half of the chapter discusses accretion experiments while second half explains the drilling simulator tests.

Chapter 4 contains the results section of thesis. It presents and explains the results of all the experiments discussed in chapter 3.

Chapter 5 presents a performance comparison of the different drilling fluids based on the results in chapter 4. The chapter also discusses the positive field trials with formate mud for ROP enhancement in Canada.

Chapter 6 presents the thesis conclusion and provides recommendations for future work.

Chapter 2: Literature Review

2.1 INTRODUCTION

To enhance the rate of penetration (ROP) in a particular drilling environment, it is important to first study the factors that contribute to slow rates of penetration. Bit balling is one of the influencing factors that limits ROP, especially in shaly formations. Therefore, the first section of this chapter discusses bit balling and methods used for its reduction. Next, the theory of electro-osmosis is introduced, along with its application in bit balling mitigation. This is followed by results from the Deep Trek experiments and introduction of chemical osmosis. Applications and dynamics of chemical osmosis are also discussed. The last section of the chapter discusses the literature related to formate fluids, their properties, environmental concerns, and their applications as HPHT fluids.

2.2 BIT BALLING

2.2.1 Introduction

Bit balling is a condition in which rock cuttings adhere to the bit surface, thereby forming a cushion between the bit and the rock and thus preventing the cutter from efficiently contacting and cutting the virgin formation. Bit balling is therefore a well-known limiter of the ROP (Dupriest and Koederitz, 2005; Remmert et al., 2007).

Once the rock is drilled and the cutting is released from the rock matrix, the radial effective stress acting on the cutting is given by the following relationship (van Oort, 1997):

$$\sigma^{eff}{}_r = P_{mud} - P_{pore} - P_{swelling} \tag{2.1}$$

where,

P_{mud} = Uniform mud pressure, which replaces the in-situ stress as the cutting is released

P_{pore} = Pore pressure

$P_{swelling}$ = Swelling pressure, which acts as a tensile force on clay platelets

According to van Oort (1997), when the in-situ stress is released from the shale cutting, swelling pressure creates a vacuum and draws water from the nearby cuttings or from water layers present on the bit surface. As a result, the cuttings begin to adhere to each other and to the surface of the bit, causing the bit to ball. The tendency of cuttings to stick to the bit is also a function of the water content of the cuttings, which is given by the Atterberg limits. As seen in Figure 2.1, the intermediate plastic zone can be referred as the balling zone. The initial water content of the shale depends on the type of shale and its clay content; if it lies in this plastic region, drilling fluid should be designed to either dehydrate the cuttings to the dry zone or hydrate them to the liquid zone. However, hydrating the cuttings to the liquid zone using dispersive mud systems can give rise to mud rheology and wellbore stability problems due to their solids-dispersing tendency. Cooper and Roy (1994) successfully demonstrated the application of electro-osmosis (discussed in detail in the next section) to reduce bit balling by dehydrating the cuttings to the dry zone. Our research is

directed toward the application of another mechanism called chemical osmosis, which works on a principle similar to electro-osmosis.

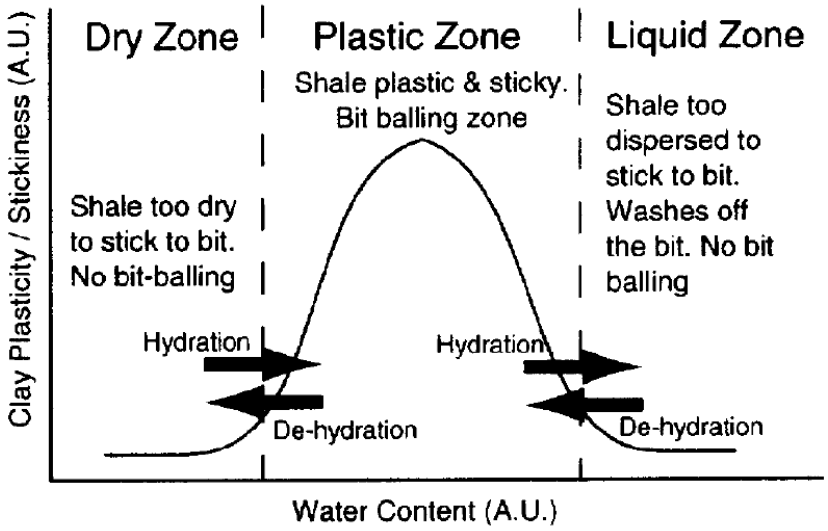

Figure 2.1: Atterberg limits showing bit balling as a function of water content (van Oort, 1997).

2.2.2 Methods of Bit Balling Reduction

A PDC bit drills the rock through its shear cutting action and is therefore more vulnerable to balling because of its tendency to generate chips. This built-up mass on the bit surface, which interferes with the effective cutting of the rock, not only reduces the ROP, but can also increase the swab & surge pressure while tripping. All of these problems result in low drilling efficiency and high drilling costs. Several studies have been conducted to understand this problem and different approaches have been adopted to mitigate the issue, but none of them has worked in all circumstances. Hariharan et al. (1998) divided these approaches into three main categories as discussed below:

1. Modification in PDC Bit and Cutter Design

Zijsling et al. (1993) claimed that the risk of primary bit balling (balling that occurs almost instantaneously after the cuttings are produced) can be minimized by providing a large cutter standoff distance in a PDC bit. A large standoff produces large cuttings that can be transported efficiently without significant contact with the bit body, thus minimizing the risk of bit balling. However, this approach weakens the bit and is only valid for a specific range of drilling parameters in certain formations.

Fear et al. (1994) suggested that bit balling could be curtailed if the open face volume (FV) of the PDC bit was maintained above a certain number. This threshold FV depended on the drilling environment and was higher for a water-based mud than for an oil-based mud. However, Wells et al. (2008) indicated that junk slot area (JSA) and FV are not solely responsible for bit cleaning and proved through a sequence of drilling tests that these parameters do not correlate with the bit performance in a controlled experiment. They claimed that bit balling in a PDC bit was rather a complex phenomenon involving multiple interacting mechanisms. Moreover, they introduced two new design factors, pinch points and junk slot shape, which should be considered to minimize balling.

Smith et al. (1995) claimed that the evacuation of rock cuttings is also affected by the thickness of the cuttings and the amount of generated friction. According to them, smoothening the surface finish of a PDC cutter (0.5 to 1 micro inches) significantly reduces the friction coefficient of the cutter and produces long thin ribbon-like cuttings, which can easily be evacuated out of the hole. This led to the introduction of polished cutter

technology for drill bits in 1995. The decrease in friction also reduces the amount of heat produced which eventually reduces wear resistance and improves bit life. Bland et al. (1997), through laboratory drilling simulator tests, showed an increase in ROP from 3ft/hr to 149ft/hr at 7500psi in balling prone shales when these polished cutters were used in conjunction with WBM (formulated with ROP enhancer). van Oort et al. (2000) suggested the use of same combination of polished cutter bit and ROP enhancer (in WBM) to minimize bit balling and reported US $3.75 million savings on 16 wells drilled in Gulf of Mexico. In recent years, considerable PDC improvements have centered around the development of these polished cutters.

Through a series of laboratory-scaled drilling experiments, Cooper and Roy (1994) minimized the balling tendency of a small PDC bit by putting a negative charge on the bit (electro-osmosis); however, the efforts to develop commercial electro-osmotic bits have been only partially successful because of challenge generating and sustaining a sufficient magnitude of negative charge on the bit during actual drilling operations. Smith et al. (1996) developed an anti-balling coating (ABC), but it is highly questionable if the low current (in the μA range) generated at the bit by this coating has any ROP enhancing effect, despite positive initial results reported by Smith. In any case, neither Smith's approach nor any other has made electro-osmosis a viable approach for ROP enhancement on a commercial scale.

2. Drilling Hydraulics Improvement

Along with other bit and mud parameters, bit hydraulics has a major influence on the drilling performance of a PDC bit. Speer (1958) directly correlated the drilling efficiency of a jet bit with the hydraulic power of the mud pump. Increasing the hydraulic power of the pump (or HSI) results in quick and prompt removal of the produced cuttings from the borehole, which enhances the ROP of the drill bit. However, in 1988, Warren et al. realized that beyond a certain HSI, hydraulics has no additional effect on cleaning of the bit and thus no longer influences ROP. Glowka (1983) and Garcia (1994) attributed this fact to certain stagnant and vortex zones under the drill bit where cuttings are trapped and cannot be removed even at high HSIs. According to van Oort et al. (2015), drill bit usually balls at low HSI (e.g. HSI less than 2.5). However, HSI cannot be independently increased, as it is governed by pump stokes and flow rates, which also directly influence the equivalent circulating density (ECD) of the drilling fluid. Note that an ECD greater than a certain value, particularly the fracture pressure, can cause serious hole problems. The effect of hydraulics on bit balling has also been studied by Holster and Kipp (1984), who concluded that gumbo-type shale such as Pierre shale cannot be drilled and stay balling-free without using water-based mud with anti-balling characteristics, regardless of the HSI used.

3. Drilling Fluid Modification

Two main types of drilling fluids are generally used to avoid bit balling in shale; however, both of them have shortcomings and are not suitable for use everywhere, as discussed below.

I. Inhibitive Water-Based Mud (WBM)

Potassium chloride (KCl) used in conjunction with partially hydrolyzed poly-acrylamide (PHPA) is considered one of the best inhibitive WBMs. Clark et al. (1976) suggested that a WBM containing KCl and PHPA can minimize borehole problems in water-sensitive shales. However, through a series of pressure transmission experiments, van Oort (1997) claimed that KCl is as poor as fresh water in stabilizing boreholes in shales. He agreed that KCl can reduce swelling pressure in clays and is thus suitable for cuttings stability (or minimizing bit balling), but it does not stop or slow down the mud pressure invasion and is thus not at all suitable for drilling stabilized holes in shales.

II. Oil-Based Mud (OBM)/ Synthetic-Based Mud SBM)

In OBM, the continuous phase is composed of liquid hydrocarbon. Due to high osmotic pressure of this continuous phase, the movement of water into the shale cuttings is restrained (thus not elevating the swelling pressure and minimizing bit balling). OBM also forms a lubricating layer on the bit surface that further helps in minimizing the balling problem. OBMs are also suitable for borehole stability as they do not allow mud pressure invasion into the formation, provided they do not have (micro-) fractures. OBMs are therefore the best mud formulations to drill quick, stable, and clean holes in shale.

However, certain problems are also associated with OBMs. van Oort et al. (2015) pointed out few of these problems as following:

- Strict environmental regulations
- Higher per barrel costs
- Difficulties in obtaining high-quality resistivity logs
- Oil emulsion blocks in tight gas sands
- Sensitivity to severe lost circulation
- Incompatibility with cement, resulting in cement problems
- High waste-disposal costs

2.3 ELECTRO-OSMOSIS

2.3.1 Theory of Electro-osmosis

Silica and alumina are two basic units of shale (clay) structure. A silica unit in itself is the tetrahedral arrangement of one silicon atom (at the center) with three oxygen atoms (at the base of the tetrahedron, each of which is again shared by two silicon atoms of adjacent units). An alumina unit is the octahedral arrangement of one aluminum atom with six oxygen atoms or hydroxyl groups (each of which is shared by two aluminum atoms of adjacent units). Depending on the type of shale (clay mineral), there are different types of silica-alumina sheets arrangements. For instance, in Kaolinite, the elementary layer

consists of one silica sheet and one alumina sheet, whereas in Montmorillonite, one alumina sheet is sandwiched between two silica sheets. According to Iwata et al. (1988), isomorphous substitution within these layers causes these clay layers to become negatively charged as aluminum replaces silicon in the silica sheet and magnesium or other divalent cation replaces aluminum in the alumina sheet. However, to balance this negative charge on the clay layer, various types of cations (Ca^{2+}, Mg^{2+}, Na^{+}) are electrostatically attached to clay sheets forming what is known as an electric double layer. When an electric potential is applied across the saturated clay, these cations are attracted to the cathode while anions move toward the anode. As these ions move, they carry their hydration shells with them (as many as 8 to 10 molecules of water e.g. for Ca^{2+}; Pálinkás et al., 1986 and Floris et al., 1994) and exert a viscous drag on the water around them. Since more mobile cations than anions are in a clay-rich shale, there is a net water flow towards the cathode. This flow is termed electro-osmosis and its magnitude depends on the electric potential gradient and the coefficient of electro-osmotic hydraulic conductivity. Different theories for quantifying this flow can be found in literature (e.g., Helmholtz (1879) and Smoluchowski (1914), Schmid (1951), and Spiegler (1958)).

2.3.2 Bit Balling Reduction through Electro-osmosis – Cooper's Work

The electro-osmosis phenomenon has been used for soil stabilization (Eggestad et al., 1983), reduction of friction (Davis et al., 1980), waste site remediation (Probstein & Hicks, 1993), shallow borehole stabilization (Titkov et al., 1961), and petroleum production (Anbah et al., 1965). Cooper and Roy were the first to introduce this mechanism for bit balling reduction (1991-1994). They claimed, through a series of drilling and indentation experiments, that if a drill bit is made cathode (negatively charged) with respect to the formation, then there is osmotic flow of water out of shale towards the bit. This water forms a thin lubricating layer over the surface of the bit and reduces the sticking tendency of the clay. It then allows the cutter to be cleaned more effectively with the available horse power, yielding a substantial increase in rates of penetration.

The experimental section of Cooper and Roy's work, including testing setup, drilling parameters, fluids specifications, and other details, can be found in Roy et al. (1991), Cooper et al. (1991), and Hariharan et al. (1998). Important results and conclusions from their study are:

1. In the presence of negative potential on the indenter, local extrusion was observed; however, compaction of clay occurred when the same indenter was made positive (Figure 2.2).

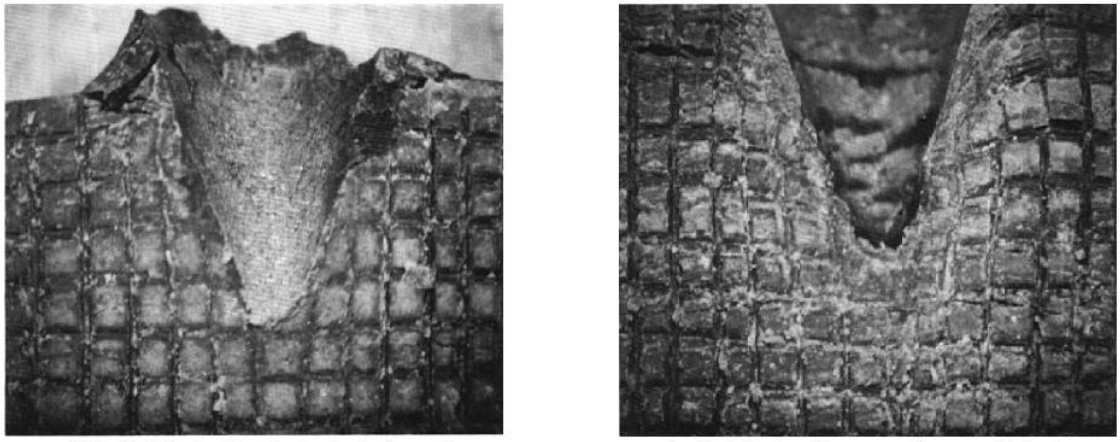

Figure 2.2: Cathodic indenter showing extrusion in clay sample (left) while compaction is observed in anodic indenter (right) (Roy et al., 1991).

2. The absolute energy required for indentation was lower for negative potential at the bit; however, it increased as the depth of the penetration increased (Figure 2.3).

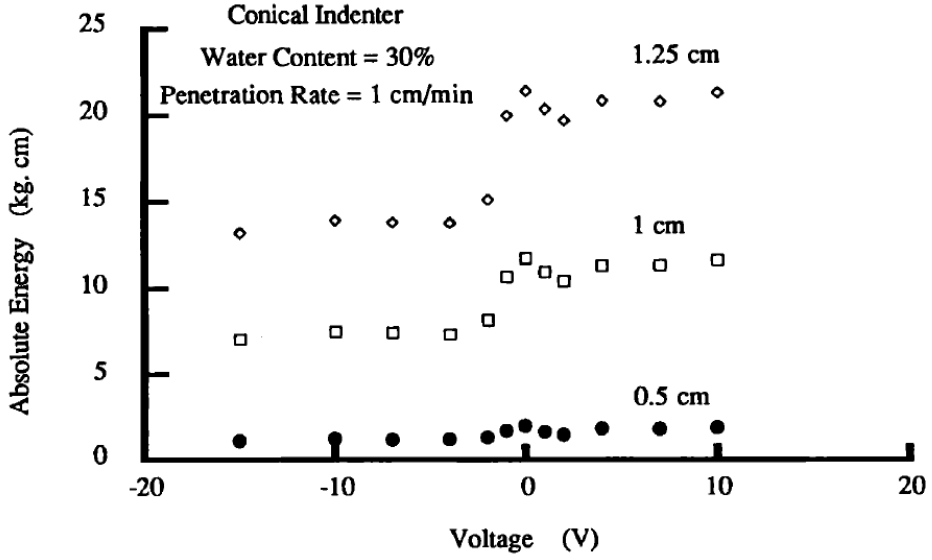

Figure 2.3: Absolute energy is plotted for various depths of penetration. Reduction in absolute energy can be seen as the bit becomes cathodic (Roy et al., 1991).

3. As seen in Figure 2.4, a certain threshold negative potential (~2V) is required to see the effect of electro-osmosis. Similarly, a certain maximum negative potential (~15V) exists, above which there is no effect.

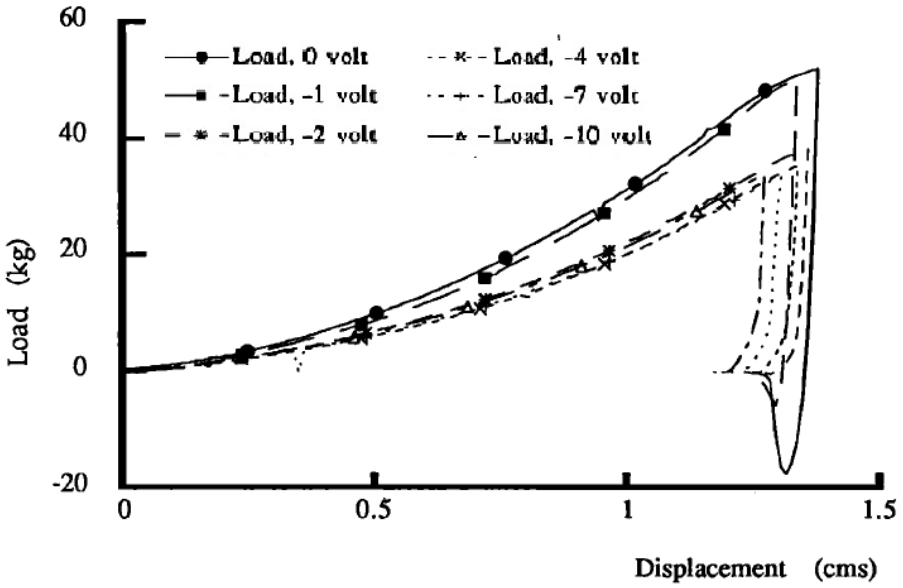

Figure 2.4: Load vs. displacement plot identifies a threshold negative potential (Roy et al., 1991).

4. Drilling experiments done on Pierre (Wellington) shale showed an almost 100% increase in ROP at higher WOBs in the presence of negative potential (10V) on the bit. Figure 2.5 shows the ROP vs. WOB data for a PDC bit drilling the Pierre shale. At low WOBs, say, below 2000N, there was no substantial compaction in the cuttings, so the bit did not ball. The process of electro-osmosis works against balling, and since, there was no balling at low WOBs, there was no appreciable effect of negative charge and both curves showed almost the same ROP. However, as the WOB was increased, compaction between the cuttings increased and the bit

started to ball. Therefore, at high WOBs, the effect of electro-osmosis came into play and enhanced ROP. Note the increase in ROP at 6000N from 10ft/hr to 18ft/hr when the negative charge was applied.

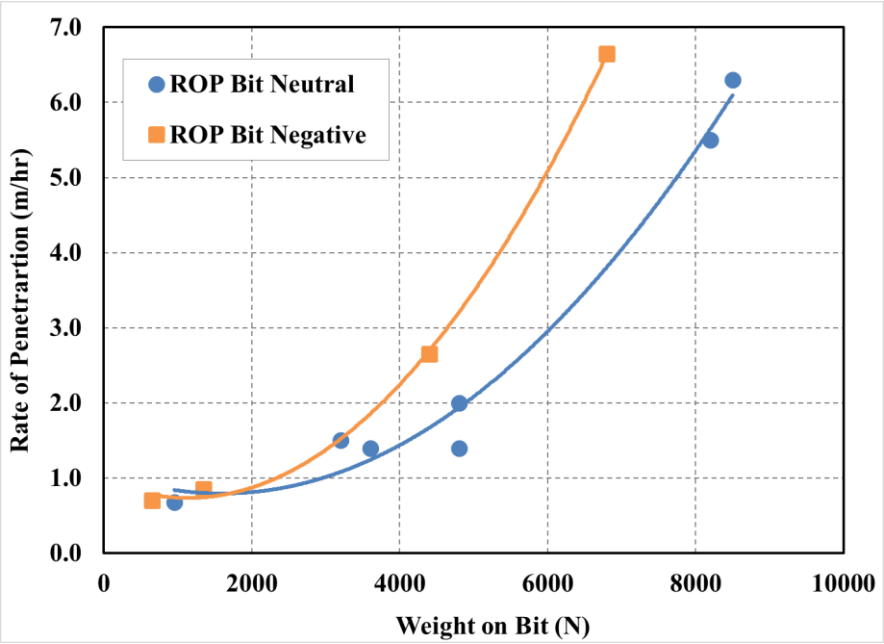

Figure 2.5: ROP vs. WOB data for negative and neutral bit (Cooper et al., 1991).

5. Figure 2.6 shows the weight comparison of the cuttings sticking to the PDC bit measured on the neutral as well as the cathodic bit. Note the substantial decrease in cuttings weight at higher WOBs.

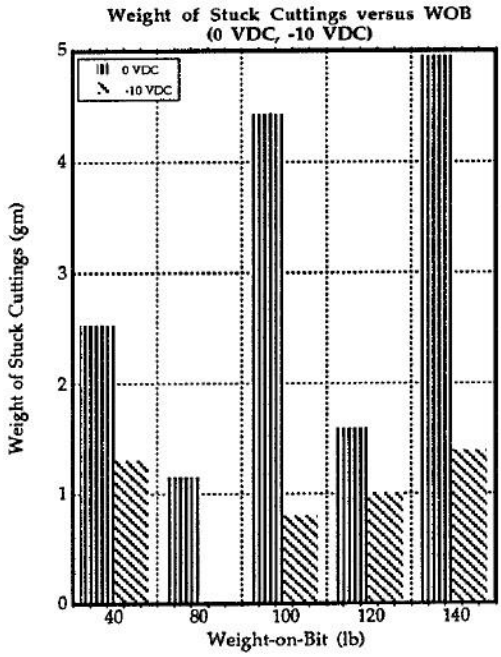

Figure 2.6: Weight comparison of stuck cuttings between cathodic and neutral bit as a function of WOB (Hariharan et al., 1998).

2.4 DEEP TREK TESTING

In 2002, the Deep Trek program was tasked to develop a drilling system tough enough to withstand the extreme conditions of deep reservoirs (temperatures greater than 347ºF and pressures higher than 10,000 psi) and economical enough to produce those deep oil and gas reserves. The research has mainly focused on increasing the rates of penetration in deep drilling and involved testing drill bits and advanced fluids under high-pressure conditions.

Figure 2.7, taken from the referenced paper, shows the ROP of a 6" PDC bit in Mancos shale as a function of WOB for different drilling muds tested during the research. Details of the concerned muds as extracted from the paper are provided in Table 2.1.

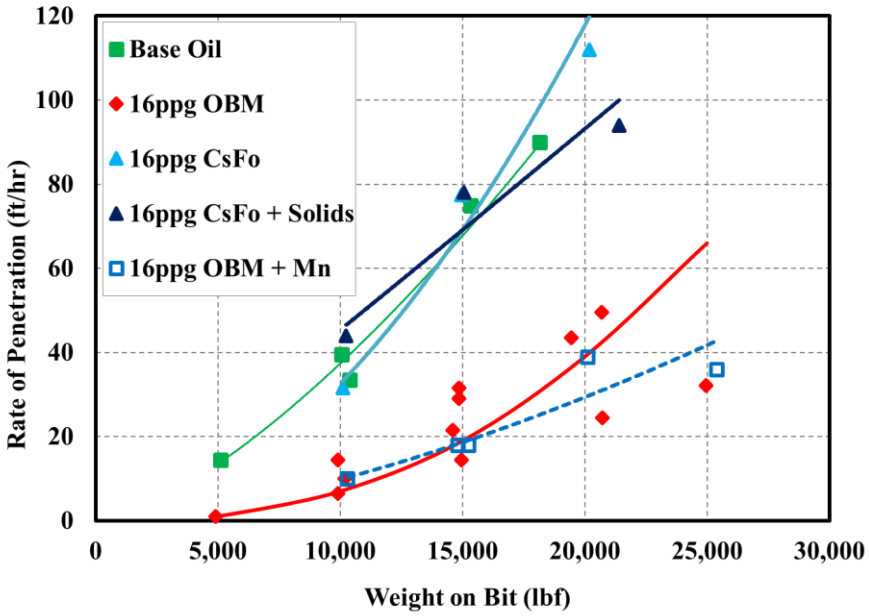

Figure 2.7: ROP vs. WOB data for various drilling fluids in Mancos shale (Black et al., 2008). Data is plotted for base oil, 16ppg OBM, 16ppg cesium formate, 16ppg cesium formate with solids, and 16ppg OBM with manganese. Details of the fluids are given in Table 2.1.

All these tests were conducted with full-scale drilling test equipment with a seven-bladed 6" PDC bit at 10,000 psi borehole pressure. Confining and overburden pressures were kept at 11,000 psi and 12,000 psi, respectively. However, both formations (Carthage limestone and Mancos shale) were drilled at a higher HSI (~5) in the cesium formate system as compared to HSI of ~2 in 16ppg OBM. The following significant conclusions can be derived from the study:

Table 2.1: Drilling fluids constituents (Judzis et al., 2007 and Black et al., 2008).

Drilling Fluids	**Constituents**
12ppg Base Oil	0.5435 bbl/bbl mineral oil - 12 ppb amidoamine emulsifier - 2.34 ppb modified FA emulsifier - 3.16 ppb lime - 4.2 ppb organoclay - 0.214 bbl/bbl calcium chloride brine - 45 ppb RevDust - 0.2 ppb XCD (Barazan D) - 189.3 ppb barite
16ppg OBM	0.5047 bbl/bbl mineral oil - 12 ppb amidoamine emulsifier - 4 ppb modified FA emulsifier – 3.89 ppb organoclay - 0.106 bbl/bbl calcium chloride brine - 35 ppb RevDust – 425.4 ppb barite
16ppg CsFo	0.97 bbl/bbl cesium formate - 2 ppb FLCA - 2 ppb suspending agent - 20 ppb calcium carbonate
16ppg CsFo + Solids	0.95 bbl/bbl cesium formate - 2 ppb FLCA - 2 ppb suspending agent - 20 ppb calcium carbonate – 20 ppb RevDust
16ppg OBM + Mn	0.5693 bbl/bbl mineral oil - 7 ppb amidoamine emulsifier - 0.4 ppb wetting agent - 1 ppb organoclay - 0.113 bbl/bbl 25% calcium chloride brine - 35 ppb RevDust – 437.8 ppb manganese tetraoxide

- As seen from Figure 2.7, cesium formate increased ROP by more than 100% compared to 16ppg OBM at higher WOBs. For instance, at around 20,000lb WOB, cesium formate drilled at approximately 115 ft/hr while 16ppg OBM drilled at 40 ft/hr. No drilling data is available for 12ppg base oil at this WOB; however, if the corresponding line is extrapolated to 20,000 lb WOB, base oil would show almost

the same ROP as 16ppg cesium formate mud. Thus, 16ppg cesium formate mud drilled as fast as the base oil mud.

- Though loading up the cesium formate mud with an extra 20ppb calcium carbonate (dark blue triangles in Figure 2.7) somewhat reduced the drilling efficiency of the mud, particularly at higher WOBs, it still maintained higher ROP than 16ppg OBM.

- The cesium formate system also showed more or less similar characteristics in Carthage limestone.

- Improvement in ROP with formate mud was seen primarily with PDC bits.

This large improvement in ROP in the presence of cesium formate can result for the by following reasons:

- *Hydraulics*: HSI maintained in cesium formate testing was almost twice as high as that in OBM testing. Higher HSI ensured better bit and hole cleaning and thus resulted in ROP improvement.

- *Bit Aggressiveness and Efficiency*: The Deep Trek team attributed this improvement in ROP to the increase in bit aggressiveness and efficiency caused by the presence of clear/low-solids cesium formate mud. They related this efficiency

to improved MSE (minimum specific energy); however, no insight into the mechanism/principle behind this effect was provided. Moreover, the better performance of cesium formate mud even in the presence of 40ppb solids was not duly explained.

- *Chemical Osmosis*: Together with better bit hydraulics and higher bit aggressiveness and efficiency, it appears that another mechanism is causing higher ROPs in cesium formate mud even in the presence of simulated solids. It is argued that this mechanism is chemical osmosis, which works similarly to electro-osmosis to draw water from the drilled cuttings out towards the drill bit, lubricating the drill bit and minimizing the sticking tendency of the rock cuttings. All these effects contribute to better instantaneous bit cleaning and thus increased ROP.

2.5 CHEMICAL OSMOSIS

2.5.1 Theory of Chemical Osmosis

Young and Mitchell (1993) defined direct and coupled flows between any two systems generated by their difference in pressure, chemical and electrical potential, and temperature. Table 2.2 below provides an overview of these flows.

Table 2.2: Overview of direct and couple flows (van Oort et al., 1996).

Flow / Force	**Hydraulic Gradient, ΔP**	**Chemical Potential Gradient, $\Delta \mu$**	**Electrical Potential Gradient, ΔE**	**Temperature Gradient, ΔT**
Fluid	Hydraulic Conduction (Darcy's Law)	Chemical Osmosis	Electro-Osmosis	Thermo-Osmosis
Solute (Ion)	Advection	Diffusion (Fick's Law)	Electro-Phoresis	Thermal Diffusion
Current	Streaming Current	Diffusion Current	Electric Conduction (Ohm's Law)	Thermo-Electricity
Heat	Isothermal Heat Transfer	Dufour Effect	Peltier Effect	Thermal Conduction (Fourier's Law)

Direct flows are given in the diagonal and are well defined by their respective laws. Coupled flows are off the diagonal. Chemical and electro-osmosis fall in the category of coupled flows as they are characterized by the movement of a fluid under a chemical and electrical potential gradient, respectively. Electro-osmosis has been explained earlier, so the following discussion will be limited to chemical osmosis.

Chemical osmosis can be defined as the movement of water molecules across a membrane system driven by a chemical potential gradient, often expressed as the difference in water activity between two systems in contact with each other. Mathematically the water activity (a_w) of a system is defined as the partial vapor pressure of water in the system divided by the standard state partial vapor pressure of water. The standard state is most

often defined as the partial vapor pressure of pure water at the same temperature. In the discussion of fluid flow, the difference in water activity acts as the indicator of flow direction: water always migrates from systems of high a_w to systems of low a_w driven by a chemical potential force that will restore chemical potential equilibrium between the two fluid systems.

2.5.2 Applications of Chemical Osmosis

Chemical osmosis is a well-known phenomenon in the oil and gas industry. In drilling fluids, this phenomenon is mainly employed to produce stable boreholes while drilling shales. Due to the hydraulic pressure gradient between drilling mud and formation (shale), water/filtrate invades the formation rock causing an increase in the swelling pressure and pore pressure, reducing effective stress. Once the effective stress reaches a certain limit shear failure of the rock may occur and the borehole may become unstable. Three basic applications of this mechanism in preventing unstable boreholes while drilling shale are discussed below:

1. Balanced Activity Oil Muds / Invert Oil Emulsion Mud

Chenevert (1970) introduced the idea of balanced activity oil-based muds to drill stable boreholes in shales. He suggested that balanced activity oil-based mud's relative vapor pressure in the drilling environment can be made equal to the relative vapor pressure of the formation (shale). Balanced activity can be achieved by increasing the salinity of the

water phase of the mud until its chemical potential is equal to that of the formation. Thus, by adjusting the water activity of an oil-continuous mud, osmotic water/filtrate transfer into the formation can be prevented and gauge boreholes can be drilled through both hard and soft shale formations provided the right mud weight is applied. Note that the oil phase acts as a perfect semi permeable membrane that will support the (surfactant-aided) transport of water but not of any solutes (e.g. salts).

2. High Salinity Water-Based Muds

A semi-permeable membrane does not exist in a WBM to support osmotic water flow; however, if a mobility difference between the molecules of water and solute exists, some sort of membrane efficiency and thus osmotic flow can be acquired (van Oort et al., 1995, 1996, 1997). The osmotic pressure between drilling fluid and formation (shale) is given by:

$$\Delta\Pi_{osmotic} = \frac{RT}{\bar{V}_w} \ln\left[\frac{a_w^{shale}}{a_w^{df}}\right] \tag{2.2}$$

where

R = Gas Constant = 8.314 J/mol K

T = Temperature

$\bar{V}_w$ = Molar Volume of Water = 18 x 10^{-6} m^3/mol at 25 ºC

a_w^{shale} = Water Activity of Formation

a_w^{df} = Water Activity of Drilling Mud (which can be reduced by increasing salinity of the mud)

To induce osmotic flow out of the shale $\boldsymbol{a_w^{shale} > a_w^{df}}$, however, the action of this osmotic pressure in case of water-based mud is weakened by a membrane efficiency σ. In the presence of oil-based mud, oil due to high capillary entry pressure acts as a perfect membrane, that is, $\sigma = 1$ (Hale et al., 1993). The effective osmotic pressure can therefore be given as:

$$\Delta\Pi_{osmotic}^{eff} = \sigma\, \Delta\Pi_{osmotic} \tag{2.3}$$

According to van Oort et al. (1996), when a shale formation is drilled with a high salinity WBM and $a_w^{shale} > a_w^{df}$, the larger mobility of water molecules compared to hydrated ions in an intact shale with narrow pores results in the osmotic flow of water from the shale to the mud. A semi-impermeable membrane thus formed due to the mobility difference of these ions is referred to a 'leaky' membrane. These leaky membranes are significantly less efficient than a perfect membrane. van Oort (1996) measured the efficiencies of several high-salinity WBMs on the order of 1% -10%. However, even at these small values of σ, effective osmotic pressure can still create the required driving force to draw water out of shales. ΔP in Figure 2.8 represents the hydraulic overbalance of the drilling mud.

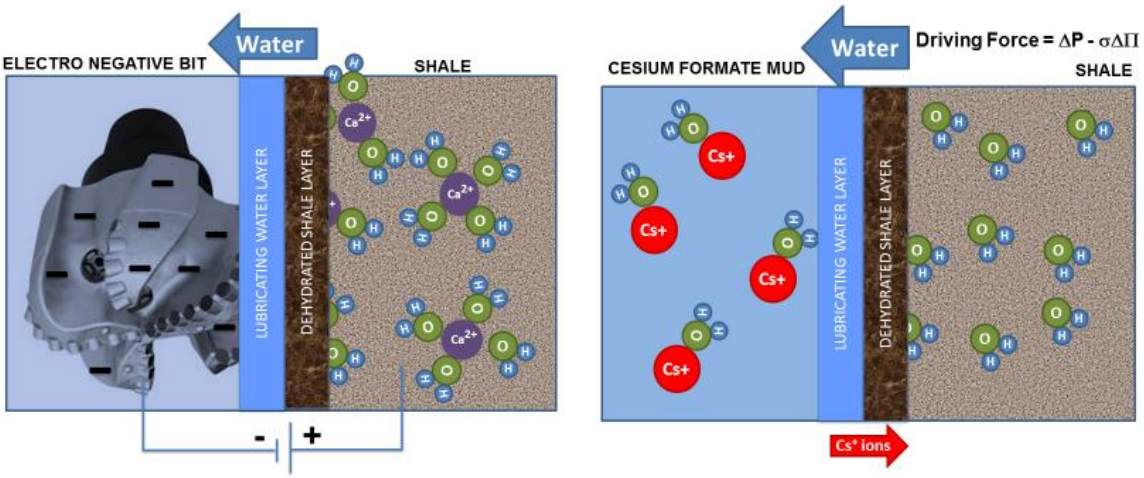

Figure 2.8: Osmotic transport of water molecules – Chemical osmosis (on the right) is analogous to electro-osmosis (on the left) (van Oort et al., 2015).

2.5.3 Dynamics of Chemical Osmosis

Sánchez et al. (2008) investigated the diffusion dynamics of water under the influence of chemical potential gradients in five different natural clays in the presence of different salts concentrations. Details of the studied clays, salt concentrations, and experimental procedures can be found in the referenced literature. In all the experiments performed on different clay samples, the diffusion coefficient of water was measured on the order of 10^{-10} – 10^{-11} m^2/s. An average value of $5.5x10^{-11}$ m^2/s will be considered in the following.

Low (1961) proposed several possible mechanisms for water adsorption in shales, including:

Hydrogen Bonding: Surface of soil minerals are composed of a layer of either oxygen or hydroxyl ion. Hydrogen bonds can form easily as oxygen attracts the positive corners and hydroxyl attracts the negative corners of water molecules.

Cation hydration: Since clay surfaces are negatively charged, so different cations are attracted to the clay surface, so is their water of hydration.

Attraction by Osmosis: Cation concentration increases as negatively charged clay surfaces are approached. This increased concentration means that water molecules tend to diffuse toward the surface in an attempt to equalize concentration

Dipole attraction: Water dipoles orient with their positive poles directed towards the negative clay surfaces, with degree of orientation decreases as distance from the surface increases.

Each mechanism gives rise to a different arrangement of water molecules. However, the diameter of a water molecule is measured to be 0.275nm. Also, Martin (1960), using a pycnometer and x-ray diffraction technique, measured the thickness of a water film (composed of three mono layers of water) in sodium montmorrilonite on the order of 1nm. Thus, on average, the thickness of a single molecular layer of water can be safely assumed to be 0.3nm.

The rate of change of a substance concentration with time ($d\varphi/dt$) due to diffusion across a concentration gradient of $d\varphi/dx$ is given by Fick's second law:

$$\frac{d\varphi}{dt} = D \frac{d}{dx}\left(\frac{d\varphi}{dx}\right) \quad (2.4)$$

Here D is the diffusivity (m^2/s) and $d\varphi/dx$ is the one-dimension concentration gradient (mol/m^4). If $\varphi\ (x=0, t)$ is kept at φ_o (original concentration), then a simple solution of this boundary problem is given by:

$$\varphi(x,t) = \varphi_0\ erfc\left[\frac{x}{2\sqrt{Dt}}\right] \quad (2.5)$$

$2\sqrt{Dt}$ in the above equation is the Diffusion Length which measures the movement of concentration front in time t. Using the water diffusion coefficient of $5.5x10^{-11}$ m^2/s (as assumed earlier), the diffusion length of the water front in one second comes out to be 14.8μm. Thus, if the average thickness of a single water layer is assumed to be 0.3nm, this movement can be translated into extraction of approximately 50,000 water molecular layers or approximately 15,000 monolayers in a second. Therefore, it appears that the dynamics of osmotic dehydration of shale by a high-salinity mud is fast enough to be relevant on the characteristic timescale of the rock cutting process. For instance, with a bit rotation speed of 60 rpm, the cutters will attack newly exposed shale formation every 1 second. Figure 2.9 shows values of the error function (equation 2.5) plotted against water front displacement (x) for different times.

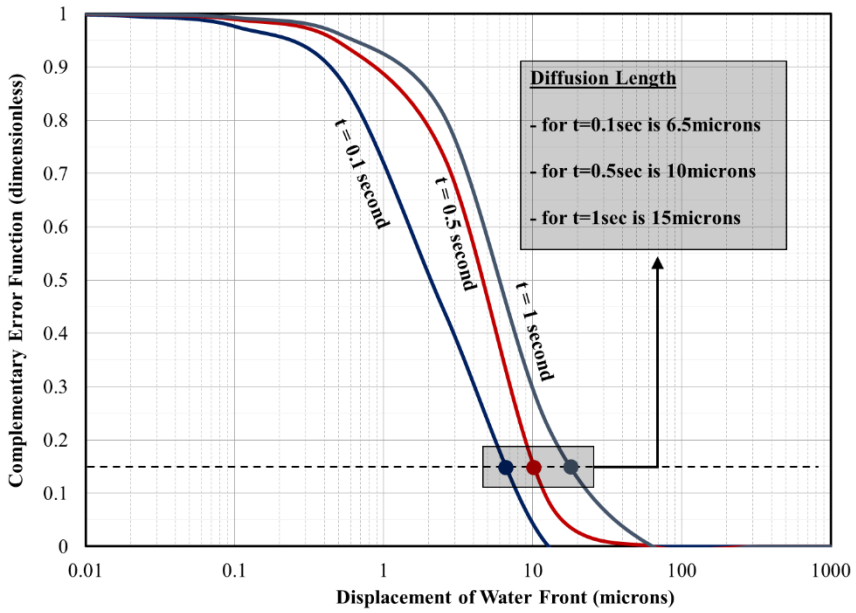

Figure 2.9: Complementary error function plotted against displacement of water front for time = 0.1sec, 0.5sec and 1sec. Diffusion lengths for each time is also shown.

2.5.4 Chemical Osmosis for Bit Balling Reduction

As discussed above, high-salinity WBMs can generate osmotic pressure high enough to draw water out of shale. The extracted water can help minimize bit balling in three ways:

1. Just as in electro-osmosis, this water forms a thin lubricating layer over the surface of the bit and reduces the sticking tendency of clay. It then allows the cutter to be cleaned more effectively with the available horse power, yielding a substantial increase in ROP.

2. Hale et al. (1993) studied the increase in shale strength caused by a reduction in shale water content. Drawing the water molecules out of shale can significantly

strengthen its outer layer, which behaves less plastically than a fully hydrated shale layer and thus is less prone to sticking and balling.

3. As shown in Figure 2.1, dehydrating the outer shale layer from the plastic zone to the dry zone can significantly reduce its plasticity and thus bit balling.

2.6 FORMATE FLUIDS

2.6.1 Introduction

Formate brines are the high-density brines formed by dissolving an aqueous solution of alkali metal salts of formic acid in water. The molecular structures of the commonly used formate salts are given below:

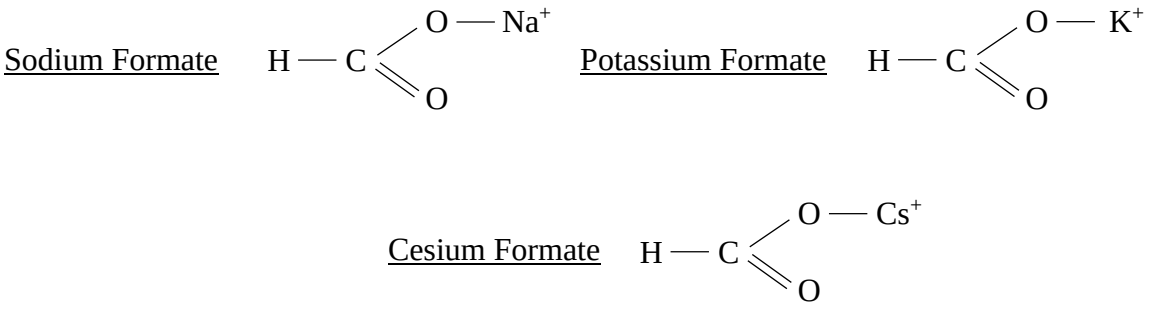

Two main reasons for selecting formate fluids in our experimental investigations are:

1. It provides continuity with previous work conducted by the Deep Trek group.
2. Formate fluids can generate very low water activity solutions and thus very high osmotic pressures, which are essentially required for the study.

Comprehensive material on the physical and chemical properties of formate brines, their compatibilities and interactions, and their field procedures is provided in the Formate Manual available online on Cabot website. However, important properties from this literature pertaining to our study are discussed below:

- Formate brines cover the entire fluid density range normally required in drilling and completion operations (Figure 2.10)

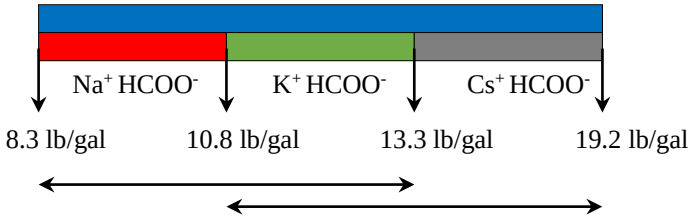

Figure 2.10: Formate brines covering the entire density range from 8.3ppg to 19.2ppg (Howard, Formate Technical Manual).

- The water activity of the concentrated brine solutions of cesium and potassium formate is approximately 0.3. Cabot has also measured the water activities of various blends of cesium and potassium formate. Figure 2.11 shows the relationship between water activity and density of the blend at 77°F.

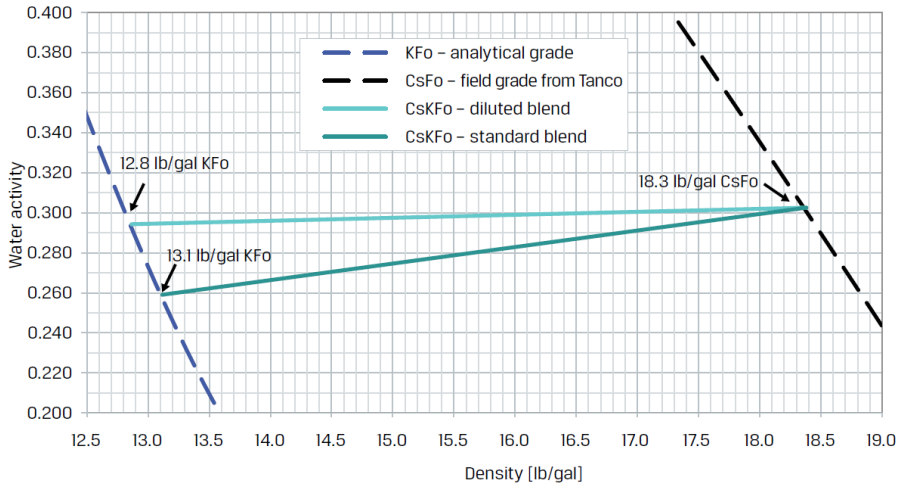

Figure 2.11: Water activity for various blends of cesium and potassium formate plotted against their density (Howard, Formate Technical Manual).

- Formate brines are compatible with most of the water-based drilling fluids and additives. Exceptions are divalent halides and barite, which form precipitate when coming in contact with formate ions. Formate brines can also have an adverse effect on the clouding glycols commonly used in some WBM for shale drilling. The formate literature should be consulted before blending these brines with any fluids/additives.

2.6.2 Environmental Concerns

Formates have been extensively tested (Gilbert et al., 2003; Zuvo et al., 2005) and are considered to be readily bio-degradable and low in toxicity for the marine environment. Gilbert et al. (2007) has pointed out some inconsistencies in global environmental regulations for formate fluids.

Formates represent low environmental hazard under OSPAR for use in the North Sea. An extensive environmental impact assessment performed by the environmental consultancy Metoc in 2003 indicated that even large accidental spills of formate brines do not cause environmental damage. Similarly, a high-resolution environmental survey was carried out in 2005, three years after drilling an exploration well with formate brine in the Barents Sea. The survey (Zuvo et al., 2005) reported minimal environmental impact caused by the discharged cuttings.

In contrast to other high-density completion fluids like zinc bromide, the transport of formate fluids is free from demanding restrictions both offshore and onshore.

The US Environmental Protection Agency (EPA) has set a maximum allowable concentration of 3% for solid particular phase (SPP) LC_{50} tests. Higher concentrations of cesium and potassium formate generate $LC_{50} > 3\%$ and are therefore beyond the tolerance level of particular test organisms. Thus, formate muds can only be used under zero-discharge conditions in the Gulf of Mexico.

2.6.3 HPHT Fluids

Because of the following characteristics, formate brines are best suited for high-pressure high-temperature (HPHT) drilling and completion applications.

- HPHT drilling and completion operations are faster and more cost-effective when drilled with formate mud. Downs (2011) reported a reduction of 30 days in completion operations of offshore HPHT wells.
- Formate fluids are clean fluids that do not damage the reservoir, thus eliminating the need for post-drilling clean-ups or stimulation treatments to remove formation damage.
- They create an ideal low-solids fluid medium and thus facilitate better reservoir visualization and definition.

Given these characteristics of formate muds, however, these fluids have not yet been accepted worldwide for drilling application. Below are the two possible reasons pointed out by van Oort et al. (2015):

- High cost of cesium formate: It is, however, possible to formulate muds by blending low-cost sodium and potassium formate with cesium formate. Details can be found in the referenced literature. Similarly, good formate characteristics can also be achieved by formulating mud with Manganese Tetroxide as a weighting agent (Al-Bagoury & Steele, 2014).
- Environmental Concerns: These concerns are discussed above in detail.

Chapter 3: Experiments - Testing Set-ups and Procedures

3.1 INTRODUCTION

As discussed in chapter 1, the basic objective of this research is to study the effect of chemical osmosis on bit balling reduction and see how this reduction enhances the rate of penetration (ROP) in an actual drilling environment. An experimental investigation of the proposed study was therefore carried out in two phases.

In the first phase, a qualitative effect on bit balling was studied using small-scale accretion tests. The primary purpose of these tests was to prove the proposed hypothesis on the laboratory scale and then pre-screen mud formulations for the second phase experiments. The next phase was then carried out in a high-pressure drilling simulator under realistic downhole drilling conditions. Large blocks of shale and limestone were drilled and the effect of chemical osmosis on ROP enhancement was studied.

To investigate the effect of chemical osmosis, different formulations of formate brine were used as drilling fluids throughout the course of this study. Details of the brines used in the experiments are discussed in the respective sections.

3.2 ACCRETION TESTS

Accretion studies have been used extensively to study the sticking tendency of clay in the presence of different drilling fluids or their additives. Even though accretion is a relatively simplistic and cost-effective method, its results generally extrapolate well to actual field practices.

3.2.1 Test Procedure

Accretion was studied in the laboratory using a rolling bar accretion test method. Tests were conducted for a variety of cesium and potassium formate solutions, details of which are provided in the next section. The steps below were followed:

1. Place a clean hollow steel bar in a mason jar containing one laboratory barrel (350ml) of drilling fluid.
2. Add 25 grams (W_1) of shale cuttings to the jar. Use ¼" bentonite tablets to simulate the effect of reactive shale cuttings.
3. Seal the lid of the jar and place it horizontally in a roller oven at 120 ºF for 30 minutes.
4. Carefully remove the bar from the jar and gently rinse off extra mud.
5. Photograph the accreted bar for qualitative analysis.
6. Scrape off adhered solids from the bar and measure their weight (W_2).

7. Allow the accreted solids to dry to a constant weight (W_3) at 220 ºF.

3.2.2 Drilling Fluids

1. Water Activities of Base Brine

Concentrated solutions of cesium formate (water activity = 0.326, density = 18.36ppg) and potassium formate (water activity = 0.260, density = 13.10ppg) were provided by Cabot Specialty Drilling Fluids. These solutions will be referred to as stock brines in the discussions ahead.

The accretion studies were first carried out in cesium formate solutions. Initially, following water activities were selected for the base brine. Table 3.1(a) shows theoretical osmotic pressures generated by the corresponding water activity brine solution of cesium formate calculated from equation 2.2 (Chapter 2).

Table 3.1 (a): Theoretical osmotic pressures against selected water activity solutions for cesium formate assuming $a_w^{shale} = 1.00$

Water Activity @ 25 ºF	**Osmotic Pressure @ 25 ºF (MPa)**
0.326	154.28
0.550	82.29
0.775	35.08
1.000	0.00

Water activity of 1.00 in Table 3.1(a) represents distilled water only with no formate brine and thus zero osmotic pressure. However, even low concentration solutions

of cesium formate (water activity on the order of 0.775) did not show any accretion at all. It was therefore decided to further investigate the water activity window between 0.775 and 1.00 and thus the solutions shown in Table 3.1(b) were selected; the table also shows the osmotic pressure of diluted solutions of cesium formate.

Table 3.1 (b): Theoretical osmotic pressures against selected water activity solutions for cesium formate assuming $a_w^{shale} = 1.00$

Water Activity @ 25 ºF	**Osmotic Pressure @ 25 ºF (MPa)**
0.900	14.50
0.955	6.34
0.970	4.19
0.987	1.80

Similarly, based on the results obtained from cesium formate, the water activities shown in Table 2.2 were selected for the potassium formate tests.

Table 3.2: Theoretical osmotic pressures against selected water activity solutions for potassium formate assuming $a_w^{shale} = 1.00$

Water Activity @ 25 ºF	**Osmotic Pressure @ 25 ºF (MPa)**
0.850	22.37
0.907	13.44
0.956	6.19
1.000	0.00

2. Preparation of Base Brine

Once the water activity of base brines for each drilling fluid was selected, the next step was to prepare the base solution. The water activity charts in the Cabot manual were used to determine the density of the solution corresponding to a particular activity. Results obtained are shown in Table 3.3.

Table 3.3: Required densities of base brines (Howard, Formate Technical Manual).

Water Activity	**Density (ppg)**
Cesium Formate Brine	
0.326	18.36
0.550	15.80
0.775	13.20
0.900	11.20
0.955	10.00
0.970	9.60
0.987	9.00
1.000	8.34
Potassium Formate Brine	
0.850	9.60
0.907	9.20
0.956	8.80
1.000	8.34

The following series of equations was then used to determine the volume of stock brine and water to prepare one laboratory barrel (350ml) of each base brine.

$$V_{stock}(lab\ bbl) = \frac{\%wt_{req} \times \rho_{req}}{\%wt_{stock} \times \rho_{stock}} \quad (3.1)$$

$$V_{water}(lab\ bbl) = \frac{\rho_{req} - (V_{stock} \times \rho_{stock})}{8.336} \quad (3.2)$$

where

V_{stock} = Required volume of stock brine to prepare 1 lab bbl of base brine

V_{water} = Required volume of distilled water to prepare 1 lab bbl of base brine

ρ_{req} = Required density of base brine from Table 3.3 in ppg

ρ_{stock} = Density of stock brine = 18.36 ppg for cesium formate
13.1 ppg for potassium formate

$\%wt_{stock}$ = Weight percentage of formate in stock brine = 79.95% for cesium formate
74.99% for potassium formate

$\%wt_{req}$ = Required weight percentage of formate = $A\rho_{req}^3 + B\rho_{req}^2 + C\rho_{req} + D$ where

	A	*B*	*C*	*D*
Cesium Formate	0.037817	-2.08025	42.3143	-229.760
Potassium Formate	0	-0.958521	36.25481	-235.455

Table 3.4 shows the calculated volume of stock brine and water required to make one lab bbl of base brine for each density solution.

Table 3.4: Volumes required for base brines.

Water Activity	**Density (ppg)**	V_{stock} **(lab bbl)**	V_{water} **(lab bbl)**
Cesium Formate Brine			
0.326	18.36	1.00	0.00
0.550	15.80	0.74	0.27
0.775	13.20	0.48	0.53
0.900	11.20	0.28	0.73
0.955	10.00	0.16	0.85
0.970	9.60	0.12	0.89
0.987	9.00	0.06	0.94
1.000	8.34	0.00	1.00
Potassium Formate Brine			
0.850	9.60	0.24	0.78
0.907	9.20	0.16	0.85
0.956	8.80	0.08	0.92
1.000	8.34	0.00	1.00

3. Preparation of Drilling Fluids

Formate brines were viscosified by adding xanthan gum (XC polymer, specific gravity = 0.75). The concentration of polymer was varied among different brine solutions to obtain roughly the same non-Newtonian viscosity, as characterized by using a plastic

viscosity (PV) and a yield point (YP) for each brine. This was intended to avoid viscosity contributions and artifacts to dispersion of cuttings and accretion tests. The target viscosity parameters (PV ~ 10 cP, YP ~ 25 lb/100ft^2) were achieved in all but the most concentrated formate solutions.

Calcium carbonate (specific gravity = 2.675) was then added to the viscosified brine to simulate the effect of solids in drilling fluid. Final fluids were prepared with 0 ppb, 15 ppb, 30 ppb, and 40 ppb concentration of solids. Table 3.5 shows the final composition of each drilling fluid, its density and rheology.

Table 3.5: Final composition of drilling fluids tested for accretion.

Water Activity	**Solids (ppb)**	**Sample Name**	**Density (ppg)**	**PV (cP)**	**YP (lb/100ft^2)**
Cesium Formate Solutions					
0.326	0	D0	18.30	28.0	17.0
	15	D15	18.37	25.1	22.0
	30	D30	18.45	27.5	18.8
	40	D40	18.51	25.0	16.0
0.550	0	C0	15.74	18.0	27.9
	15	C15	15.85	19.4	29.2
	30	C30	15.98	19.2	24.5
	40	C40	16.06	20.5	25.9
0.775	0	B0	13.15	10.2	26.0
	15	B15	13.30	10.7	25.1
	30	B30	13.46	10.9	25.8
	40	B40	13.57	11.0	28.0

Table 3.5(continued): Final composition of drilling fluids tested for accretion.

Water Activity	Solids (ppb)	Sample Name	Density (ppg)	PV (cP)	YP (lb/100ft^2)
0.900	0	Ab0	11.16	8.1	25.7
	40	Ab40	11.66	9.1	24.8
0.955	0	Aa0	9.97	8.2	25.0
	40	Aa40	10.52	8.4	26.2
0.970	0	Aa”0	9.57	7.8	25.6
	40	Aa”40	10.14	8.0	23.6
0.987	0	Aa’0	8.98	7.5	27.2
	40	Aa’40	9.57	8.5	27.4
1.000	0	A0	8.31	8.5	27.0
	15	A15	8.54	9.4	28.0
	30	A30	8.78	8.9	27.0
	40	A40	8.93	9.0	32.4
Potassium Formate Solutions					
0.850	0	D0	9.57	9.2	26.0
	40	D40	10.14	11.0	31.0
0.907	0	C0	9.18	9.0	27.2
	40	C40	9.76	8.9	26.9
0.956	0	B0	8.78	8.5	30.0
	40	B40	9.38	9.8	31.0
1.000	0	A0	8.31	7.5	26.0
	40	A40	8.94	7.3	25.0

3.2.3 Quantitative Measurements

Once all the drilling fluids were prepared, each was tested separately for accretion according to the procedure outlined in section 3.2.1 and W_1, W_2, and W_3 were measured. Percentage accretion was then calculated from the dry weight of accreted solids using the following relationship (De Stefano and Young, 2009):

$$\% \, Accretion = \frac{W_3}{\left[\frac{\{100 - M_i\}}{100}\right] \times W_1} \tag{3.3}$$

where

M_i = Water content of unexposed bentonite tablets which in our case was 0.1

W_1 = Weight of the cuttings added to the jar = 25 gm

W_2 = Weight of the wet cuttings scrapped off the bar

W_3 = Weight of the dried cuttings

Similarly, the moisture content of agglomerated solids was calculated from

$$\% \, Moisture = \frac{W_3 - W_2}{W_2} \times 100 \tag{3.4}$$

3.3 DRILLING SIMULATOR TESTS

The second phase of our experimental investigation was carried out in a high-pressure drilling simulator (Figure 3.1) located at Hughes & Christensen laboratory of

Baker Hughes. This downhole simulator can drill 20” diameter cores of rock confined under 15,000 psi at a borehole pressure of 10,000 psi using up to 12¼” drill bits. A detailed description of the simulator can be found in the literature (Ledgerwood & Kelly, 1991).

3.3.1 Rock and Drill Bit Specifications

Mancos shale and Carthage limestone were selected for the study and their rock samples were cut into cylindrical cores 36¼” in length and 15½” in diameter to be used in the simulator. Other basic properties of these rocks are given in Table 3.6. Drilling was carried out with a 5-bladed 8¾” PDC bit at a bottom-hole pressure of 6,000 psi.

Figure 3.1: Photographs of full-scale Drilling Simulator set-up.

Table 3.6: Basic properties of the drilled formations.

Property	Manos Shale	Carthage Limestone
Bulk Density	2.54 g/cm^3	2.62 g/cm^3
Unconfined Compressive Strength	9.8 ksi	13 ksi
Porosity	7.9 %	1.7 %
Permeability	-	0.002 micro Darcy

3.3.2 Drilling Procedure and Fluids Details

As the downhole simulator is a large machine, a single drilling run in the simulator required around 50 bbl of drilling fluid. Depending on the fluid used, the whole simulator testing sequence was divided into six drilling cycles, as shown in Table 3.7.

Table 3.7: Testing sequence for drilling simulator – Theoretical osmotic pressures are calculated assuming $a_w^{shale} = 1.00$

Cycle	Base Fluid	Mud Type	Water Activity	Solids Content (ppb)	Density (ppg)	Osmotic Pressure (MPa)
1	Fresh Water	Low Mud Weight	1.000	-	9.5	0.000
2	Formate Mud	Low a_w – Low Solids	0.250	10	15.7	190.814
3		Low a_w – High Solids	0.250	40	15.7	190.814
4		High a_w – Low Solids	0.825	10	11.2	26.479
5		High a_w – High Solids	0.825	40	11.2	26.479
6	Fresh Water	High Mud Weight	1.000	-	16.0	0.000

Formate mud used in the simulator testing was a blend of cesium and potassium formate; 50 bbl of each blend, low water activity (0.25) and high water activity (0.825), was provided by Cabot Specialty Drilling Fluids. The blends were later viscosified by adding XC polymer, and depending on the quantity required for a respective cycle of drilling, solids (calcium carbonate) were added accordingly.

Each cycle given in Table 3.7 was composed of two tests, one in each formation. Thus, 12 tests in six cycles were performed. Cycles 1 and 6 were reference baseline tests that were run in low and high mud weight fresh-water muds, respectively. Data obtained from Cycle 1 (9.5 ppg mud) were used in performance comparison with Cycles 4 and 5 (11.2 ppg muds) and similarly Cycle 6 (16 ppg mud) data were used for Cycles 2 and 3 (15.7 ppg muds).

Cycle 2 represented the low water activity (high salinity) formate blend test obtained with 10 ppb of calcium carbonate. After completion of Cycle 2, an additional 30 ppb of solids were added to the mud and drilling for Cycle 3 was carried out. Once the low water activity cycles were completed, the whole mud system was switched with Cycle 4 mud, which represented the high water activity (low salinity) formate blend with low solids concentration (10 ppb). Similarly, at the end of Cycle 4, an extra 30 ppb of calcium carbonate were added to the used mud to drill for Cycle 5.

PVs and YPs were measured at the start of each test. Table 3.8 gives the rheological properties of the mud used in each test.

Table 3.8: Measured PVs and YPs for each downhole simulator test.

Cycle	Base Fluid	Mud Type	Rock	Test No.	PV (cP)	YP (lb/100ft^2)
1	Fresh Water	Low Mud Weight	Carthage	01	15	15
			Mancos	02	15	14
2	Formate Mud	Low a_w – Low Solids	Carthage	03	15	13
			Mancos	04	14	12
3		Low a_w – High Solids	Carthage	05	14	12
			Mancos	06	15	10
4		High a_w – Low Solids	Carthage	07	12	19
			Mancos	08	13	18
5		High a_w – High Solids	Carthage	09	12	16
			Mancos	10	13	15
6	Fresh Water	High Mud Weight	Carthage	11	11	64
			Mancos	12	11	64

3.3.3 Drilling Parameters

As is evident from Table 3.8, Carthage was drilled first in each cycle, followed by Mancos. Drilling was always initiated at a lower weight on bit (WOB), which was progressively increased as long as the torque produced in the drilling assembly remained within operational limits. The values of the basic drilling parameters used in each test are given in Table 3.9. In each drilling test, 30" of the core was drilled and properties like ROP, WOB, torque, and specific energy were continuously recorded. Nozzle sizes for the bit

were selected in such a way that HSI for every mud weight was kept close to 2.0. Table 3.10 shows the hydraulics for each test.

Table 3.9: Basic drilling parameters for downhole simulator tests.

Drilling Parameter	Value
Mud Flow Rate	460 gpm
Rotary Speed	60 RPM
Torque	< 10,000 ft.-lbs.
Bottom-hole Pressure	6,000 psi
Drilling Mode	Constant WOB (WOB controlled)
Weight on Bit	Carthage: 10, 20, 30, 40, 50 k-lbs. Mancos: 5, 15, 25, 35 k-lbs.

Table 3.10: Drilling Hydraulics for downhole simulator tests.

Cycle	Base Fluid	Mud Type	Rock	Test No.	Hydraulic Horsepower	HSI
1	Fresh Water	Low Mud Weight	Carthage	01	120.596	2.005
			Mancos	02		
2	Formate Mud	Low a_w – Low Solids	Carthage	03	122.509	2.037
			Mancos	04		
3		Low a_w – High Solids	Carthage	05	122.509	2.037
			Mancos	06		
4		High a_w – Low Solids	Carthage	07	120.375	2.001
			Mancos	08		
5		High a_w – High Solids	Carthage	09	120.375	2.001
			Mancos	10		
6	Fresh Water	High Mud Weight	Carthage	11	124.850	2.076
			Mancos	12		

Chapter 4: Experimental Results

4.1 INTRODUCTION

Results obtained from each set of experiments (mentioned in chapter 3) are given and explained separately in this chapter. First, the qualitative results of accretion tendencies of the studied mud system are discussed. This is followed by the quantitative analysis of the accretion tendencies. Next, the drilling data obtained from all the cycles of drilling simulator tests are presented. Each cycle is discussed separately and data corresponding to each test are represented in the form of a rate of penetration (ROP) vs. weight on bit (WOB) graph.

4.2 ACCRETION TESTS

Results from the accretion experiments can be divided into two categories:

1. Qualitative results
2. Quantitative results

Each is discussed in detail in the following paragraphs.

4.2.1 Qualitative Analysis

As seen in the test procedure given in section 3.2.1 of chapter 3, once the steel bar was taken out of a particular drilling fluid, it was photographed for the qualitative analysis. Accretion tests were performed simultaneously for different water activity muds and are thus photographed together. Figure 4.1 shows the accreted bar for different water activity solutions of cesium formate.

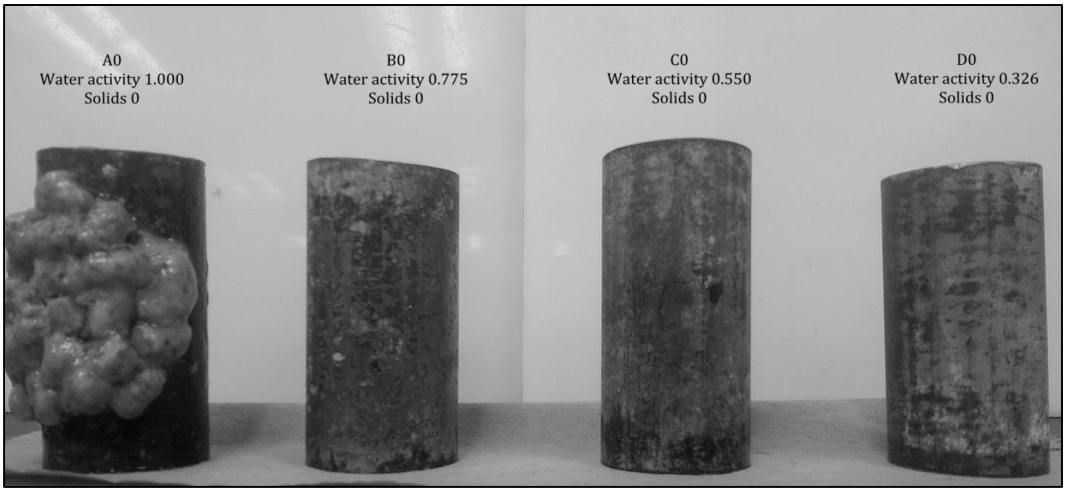

A. Zero concentration of solids

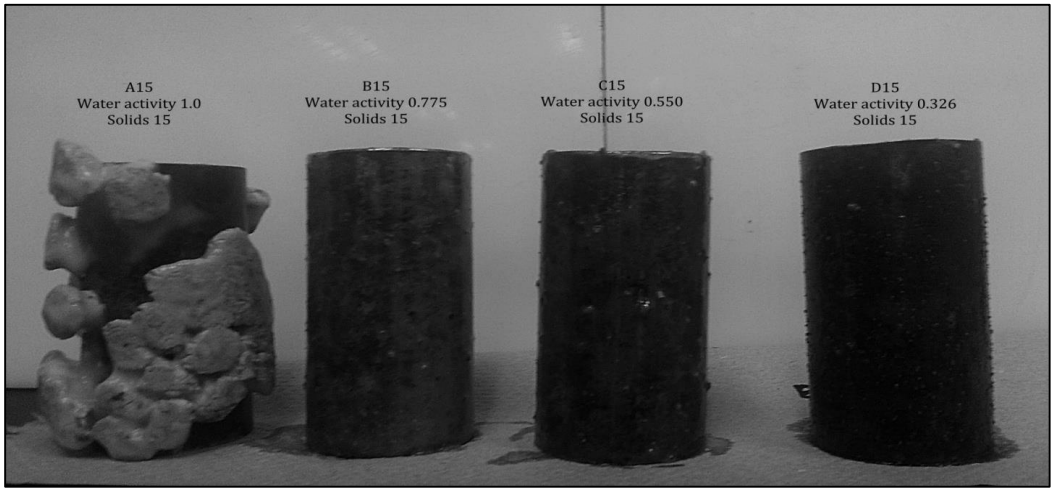

B. 15ppb concentration of solids

Figure 4.1

C. 30ppb concentration of solids

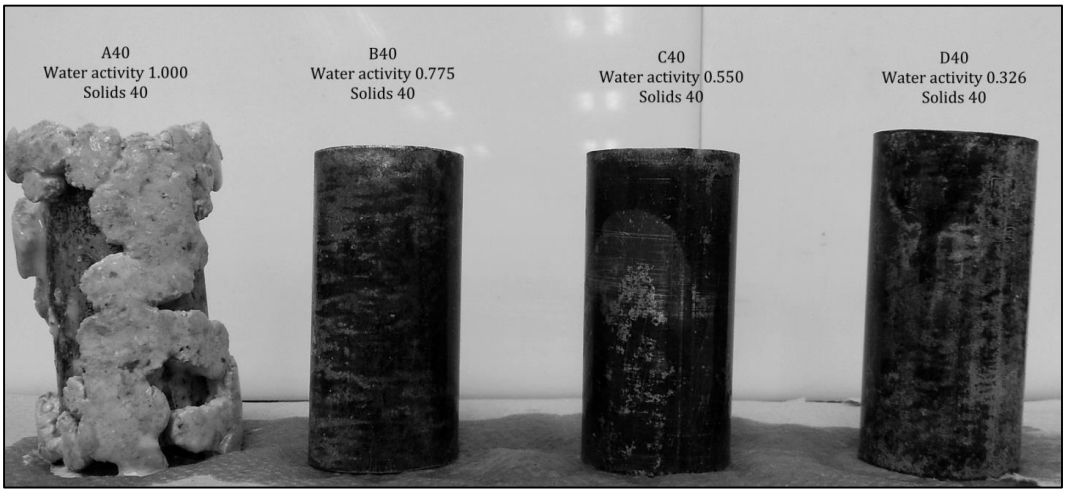

D. 40ppb concentration of solids

Figure 4.1: Accretion photographs showing the effect of cesium formate mud. Formate concentration increases (or water activity decreases) from left to right and solids concentration increases from top to bottom.

The concentration of cesium formate increases as we move left to right in Figure 4.1, the rightmost being the most concentrated solution. It is quite clear from Figure 4.1 (A to D) that while the steel bar showed accretion of shale cuttings in the presence of fresh water mud (water activity = 1.00), there was no accretion even in the most diluted solution

of cesium formate (water activity = 0.775), regardless of the solids concentration. It was therefore decided to study considerably lower concentration solutions of cesium formate (corresponding to water activities greater than 0.775). Figure 4.2 shows pictures for these diluted solutions at zero and 40ppb solids concentration.

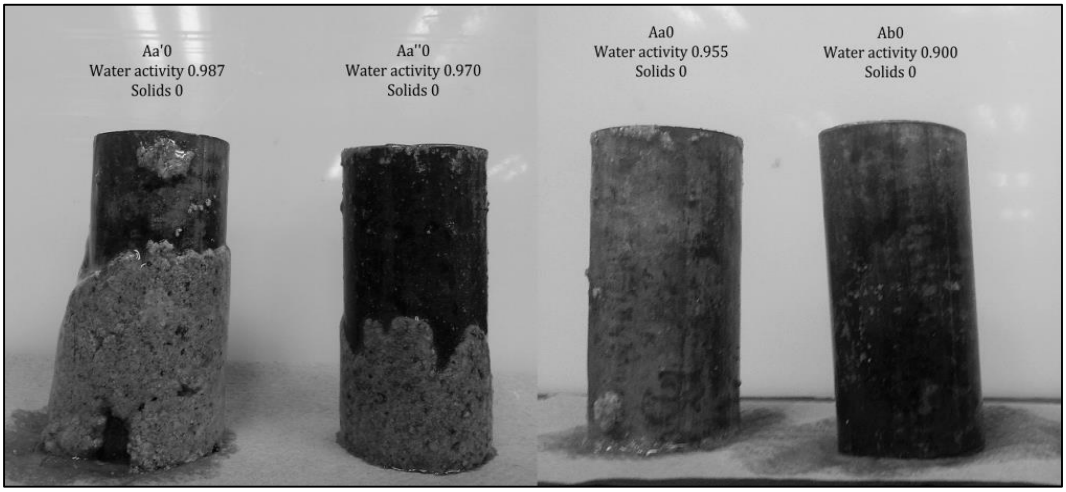

A. Zero concentration of solids

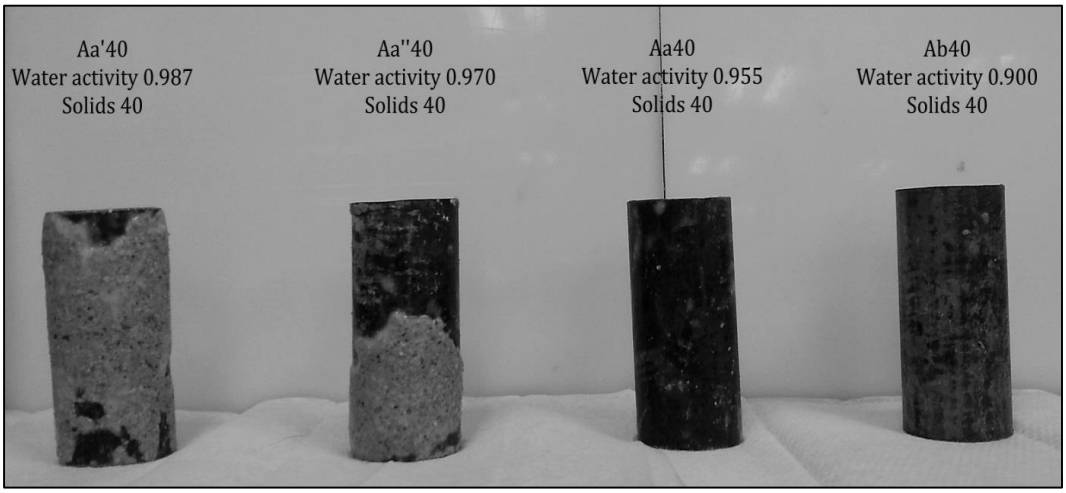

B. 40ppb concentration of solids

Figure 4.2: Accretion photographs for diluted cesium formate mud formulations for zero and 40ppb solids concentration.

As the formate concentration in the mud increases from left to right in Figure 4.2 (A), the accretion tendency of the steel bar decreases. A similar trend continues when

40ppb of solids are added to the same mud (Figure 4.2B), the only difference being the weight of the accreted shale, which is higher when the solids concentration is higher. Similarly, when potassium formate was used to prepare the base brine, the accretion tendency of the steel bar decreases with an increase in formate concentration. Figure 4.3 shows the qualitative comparison among different concentration solutions of potassium formate.

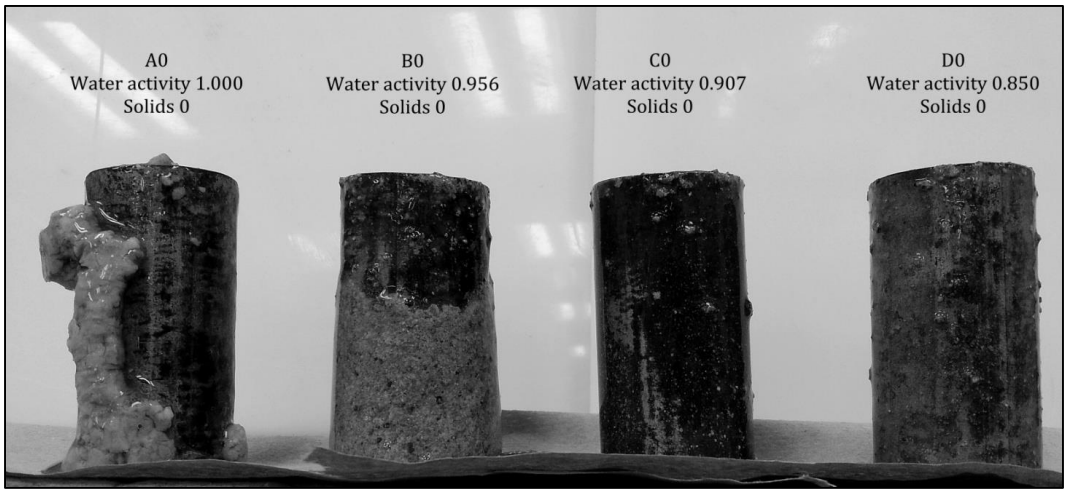

A. Zero concentration of solids

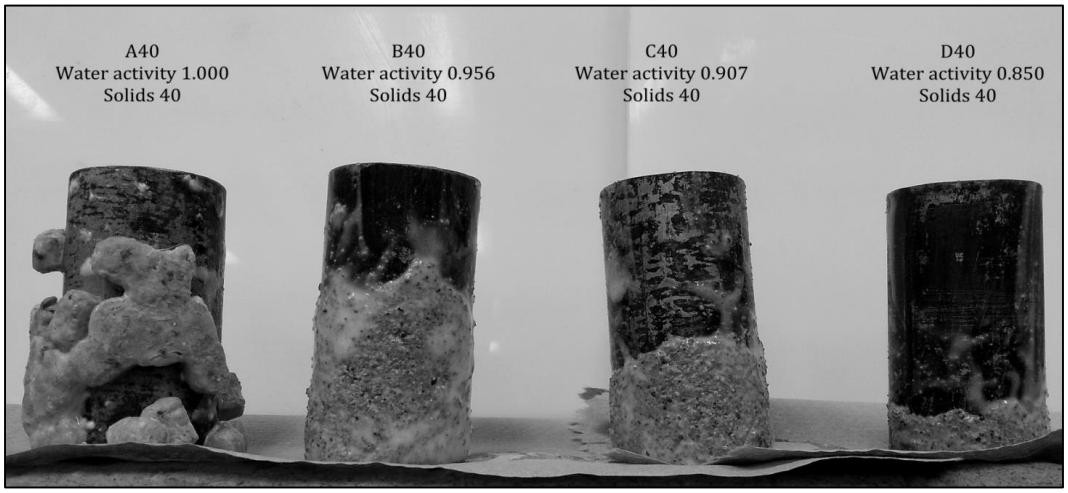

B. 40ppb concentration of solids

Figure 4.3: Accretion photographs showing the effect of potassium formate mud for zero and 40ppb solids concentration

4.2.2 Quantitative Analysis

Quantitatively, the accretion percentage is measured through equations 3.3 and 3.4 in Chapter 3. Table 4.1 provides numerical values of the percentage accretion and percentage moisture in the shale cuttings under the influence of all studied fluids.

Table 4.1: Measured values of accretion percentage for all the studied fluids.

Water Activity	Solids (ppb)	Sample Name	Density (ppg)	Measured Accretion (%)	Measured Moisture (%)
Cesium Formate Solutions					
0.326	0	D0	18.30	0.0	-
	15	D15	18.37	0.0	-
	30	D30	18.45	0.0	-
	40	D40	18.51	0.0	-
0.550	0	C0	15.74	0.0	-
	15	C15	15.85	0.0	-
	30	C30	15.98	0.0	-
	40	C40	16.06	0.0	-
0.775	0	B0	13.15	0.0	-
	15	B15	13.30	0.0	-
	30	B30	13.46	0.0	-
	40	B40	13.57	0.0	-
0.900	0	Ab0	11.16	0.0	-
	40	Ab40	11.66	0.0	-
0.955	0	Aa0	9.97	0.0	-
	40	Aa40	10.52	0.0	-

Table 4.2(continued): Measured values of accretion percentage for all the studied fluids.

Water Activity	Solids (ppb)	Sample Name	Density (ppg)	Measured Accretion (%)	Measured Moisture (%)
0.970	0	Aa"0	9.57	9.8	71.4
	40	Aa"40	10.14	14.2	53.6
0.987	0	Aa'0	8.98	53.8	58.3
	40	Aa'40	9.57	67.6	46.7
1.000	0	A0	8.31	60.4	61.5
	15	A15	8.54	88.0	55.6
	30	A30	8.78	89.3	55.5
	40	A40	8.93	81.8	56.2
Potassium Formate Solutions					
0.850	0	D0	9.57	0.0	-
	40	D40	10.14	4.0	85.0
0.907	0	C0	9.18	0.0	-
	40	C40	9.76	16.4	59.8
0.956	0	B0	8.78	18.7	70.6
	40	B40	9.38	22.7	58.9
1.000	0	A0	8.31	36.4	50.0
	40	A40	8.94	58.2	61.4

Numerical data tabulated above are represented as bar graphs in Figure 4.4. As is Figures 4.1 through 4.3, Figure 4.4 also shows maximum accretion in the presence of distilled water (water activity = 1.00).

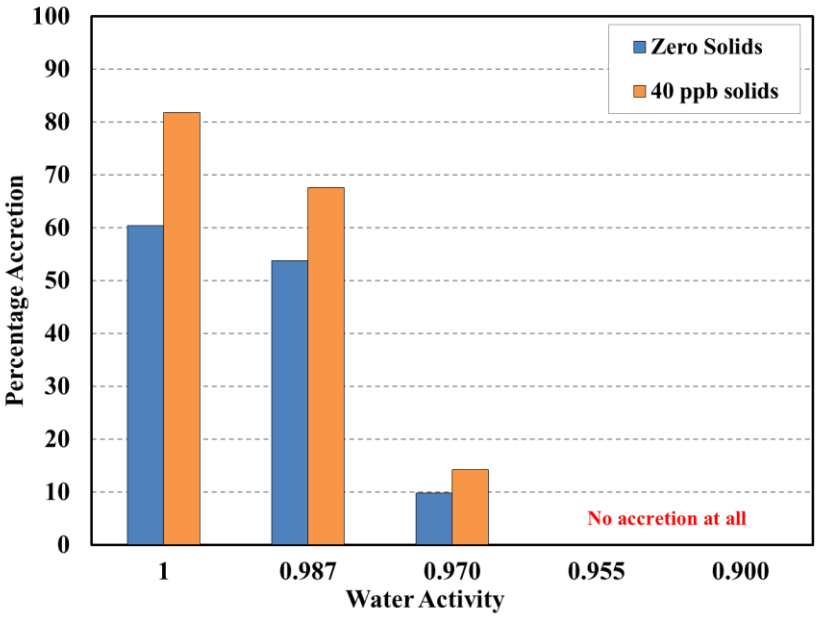

A. Cesium formate accretion tendencies

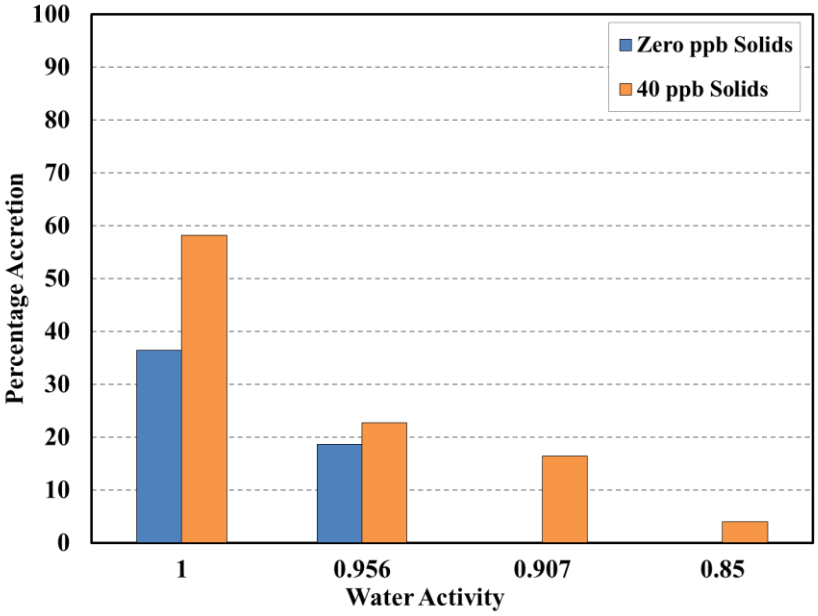

B. Potassium formate accretion tendencies

Figure 4.4: Bar chart showing percentage accretion of shale cuttings for various water activity solutions of cesium and potassium formate in the presence of zero and 40ppb concentration of solids.

The accretion tendencies are reduced as the formate concentration (cesium or potassium formate) increases in the mud. In each solution tested, the accretion percentage is higher for the 40ppb solids than the no solids solution. While a 0.85 water activity solution of potassium formate reduced accretion to less than 5%, a 0.955 water activity solution of cesium formate completely eliminated the sticking tendency of cuttings regardless of the solids concentration.

4.3 DRILLING SIMULATOR TESTS

Raw data obtained from a simulator test (Test 4 is shown as an example) are shown in Figure 4.5. Data were recorded over time (time interval = 0.25 seconds) and were reported in an Excel format at the end of each test. In each drilling test, approximately 30" of the rock formation was drilled and depending on the rock and fluid tested, corresponding number of data points (1200 – 2400) were obtained. Data represented in Figure 4.5 were obtained at the end of Test 04, when Mancos shale was drilled with low water activity and low solids formate mud. The first 70 to 80 seconds in this test represent starting up the machine and the mud pumps. Once everything was running smoothly, the actual drilling was carried out. Each drilling test was then divided into two similar halves.

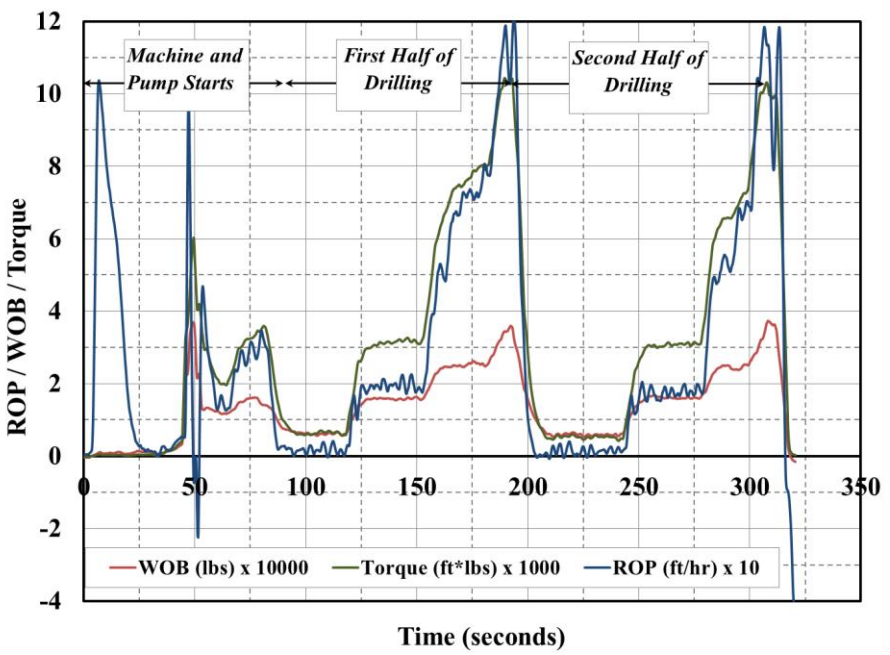

Figure 4.5: Raw (un-processed) drilling data for Test 4 as obtained from downhole simulator. ROP, WOB, and torque are plotted against drilling time.

For instance, in the given test, the first half started at around the 80th second when drilling was initiated at 5000 lbs. WOB. After attaining a constant ROP, WOB was increased to 15000 lbs. at approximately 125 seconds and then to 25000 lbs. after 155 seconds. The last step was supposed to be at 35000 lbs.; however, at such a high WOB, the torque generated in the assembly crossed the maximum operational limit of 10,000 ft.-lbs. (see green line at around the 180th second); therefore, the first half was terminated at this point. The next half was carried out in a similar way to confirm the repeatability of the data. The WOB and ROP data, obtained from the simulator tests, were given against time. However, for the purposes of this study, ROP was to be plotted against WOB for each test. If this was done directly from the raw data, the curve shown in Figure 4.6 is obtained.

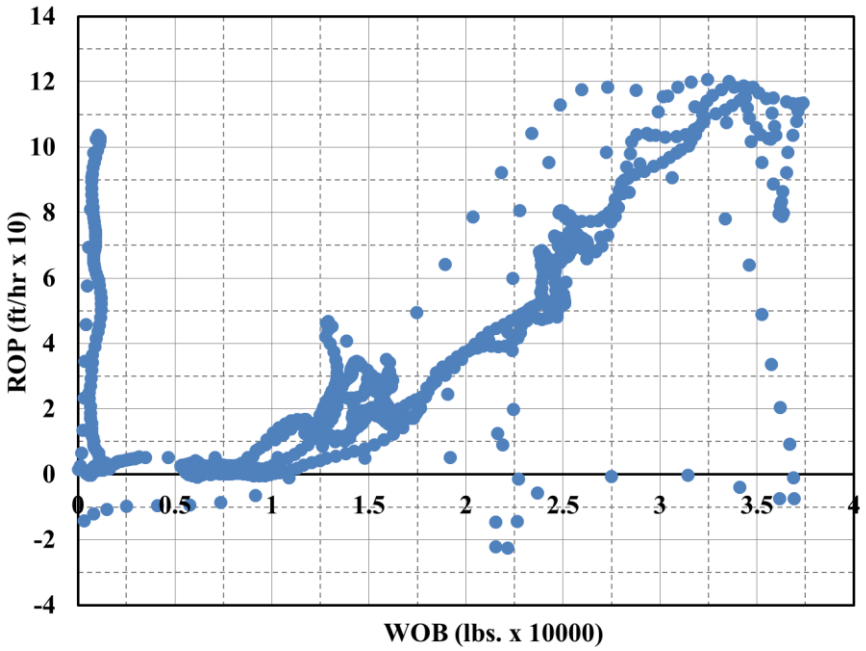

Figure 4.6: ROP vs. WOB curve obtained from raw data of downhole simulator Test 4.

Therefore, these data had to be processed before making comparative conclusions among different fluids.

4.3.1 Processing the Raw Data

The following four steps were taken to process the raw data:

1. WOB and ROP data for different time points were first grouped together and sorted in the ascending order of WOB.
2. Moving averages were then calculated with each 10 consecutive data points.

3. Abnormal data points corresponding to starting up and shutting down the drilling simulator were then ignored. Examples included negative ROPs or overly high ROPs at negligible WOBs or overly low ROPs at substantially high WOBs.

4. A second degree trend line was then fitted to the plotted data. The regression coefficient of this line was kept close to unity. The quadratic equation obtained from this line was then used to represent a certain test in making comparative analysis among different tests.

Figure 4.7 represents the curve obtained from the processed data of test 4. The same steps were followed to process the raw drilling data obtained from all six cycles performed on the drilling simulator. The results obtained from these cycles are discussed individually in the next section.

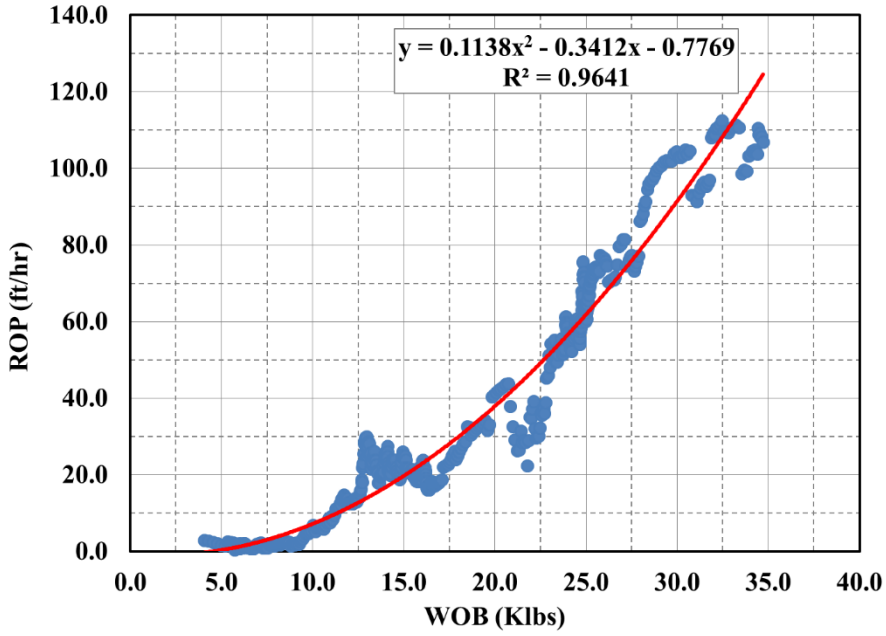

Figure 4.7: ROP vs. WOB curve obtained from the processed data of downhole simulator Test 4. A second degree regression line is also fitted to the curve.

4.3.2 Results Cycle 1 – 9.5ppg Baseline (Fresh Water) Mud

As discussed previously, each cycle was composed of two tests, one in each formation: Carthage Limestone and Mancos Shale. The mud used in this cycle was 9.5ppg fresh-water WBM with the PV and YP of about 15cP and 15lb/100ft^2, respectively. The primary purpose of this cycle was to establish the drilling parameters for formate testing. However, data obtained from this cycle were later used for comparison purposes with 11.2ppg formate mud cycles (Cycles 4 and 5).

Figure 4.8 shows the ROP vs. WOB data obtained from drilling Carthage limestone in cycle 1.

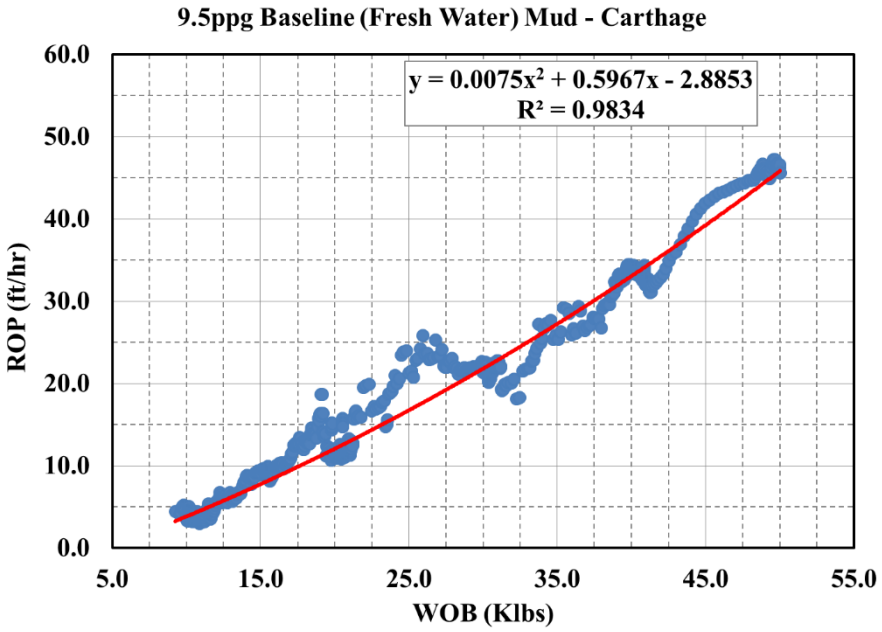

Figure 4.8: ROP vs. WOB data for Test 1 – Carthage limestone drilled with 9.5ppg baseline (fresh water) mud. A regression line with $R^2 = 0.9834$ is fitted to the data.

Drilling was initiated at 10,000 lbs., however at this WOB, the bit hardly penetrated the formation (ROP was less than 5 ft/hr). As the WOB was progressively increased to 50,000 lbs., ROP also increased with a maximum recorded ROP of 47 ft/hr. A trend line with R^2 = 0.9834 was fitted along the curve to represent the data.

ROP vs. WOB data obtained by drilling Mancos shale with the same mud are represented in Figure 4.9. For shale, WOB ranged from 5000 lbs. to a maximum of 35000 lbs. ROP started at around 5 ft/hr at low WOB but, unlike limestone, here ROP increased to a maximum of 115 ft/hr at higher WOBs. A second degree trend line was fitted to the curve; its regression coefficient, as indicated on the plot, was 0.968.

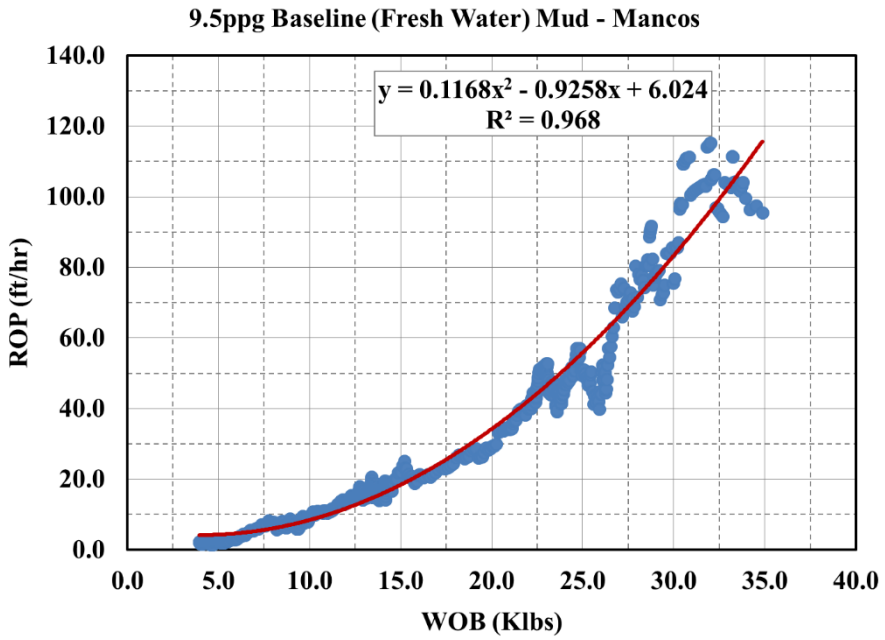

Figure 4.9: ROP vs. WOB data for Test 2 – Mancos shale drilled with 9.5ppg baseline (fresh water) mud. A regression line with R^2 = 0.968 is fitted to the data.

4.3.3 Results Cycle 2 – 15.7ppg Formate Mud / Low Solids (10ppb)

Cycle 2 represented concentrated formate mud having water activity of 0.25 and a solids (calcium carbonate) concentration of 10ppb. This 15.7ppg mud had a PV of 14 – 15cP and YP of 12 – 13lb/100ft^2. Similar to the first cycle, a drilling test was first conducted in Carthage limestone and then in Mancos shale.

Figure 4.10 represents test 3, which was conducted with cycle 3 mud in Carthage. WOB stops were made at 10, 20, 30, and 40 k-lbs. A maximum ROP of 34 ft/hr was recorded at the highest WOB. The R^2 value for the fitted trend line was 0.9776.

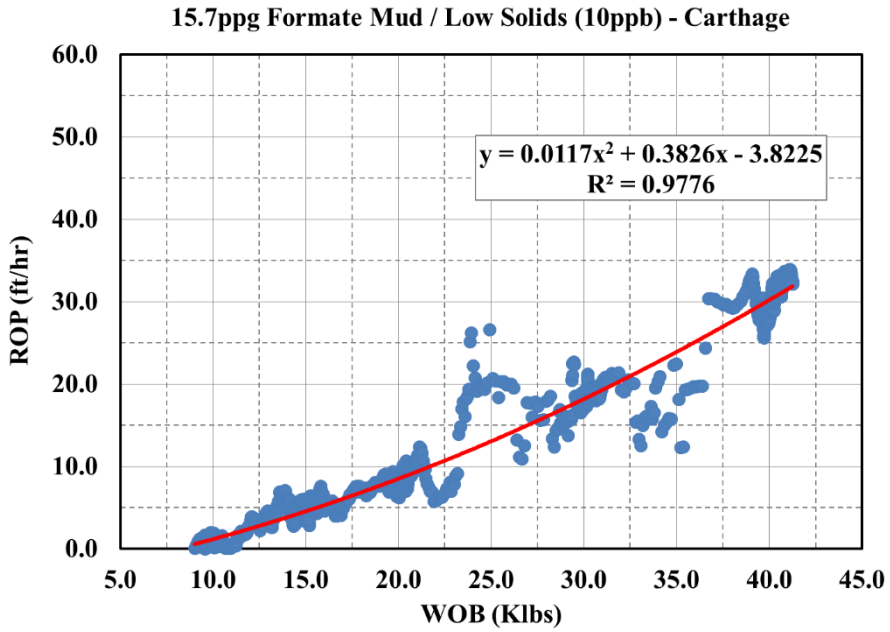

Figure 4.10: ROP vs. WOB data for Test 3 – Carthage limestone drilled with 15.7ppg formate mud / low solids (10ppb). A regression line with $R^2 = 0.9776$ is fitted to the data.

Drilling data from test 4 when Mancos was drilled with the same mud are shown in Figure 4.11. A maximum of 35k-lbs. of WOB was achieved during the drilling; however, only a small number of available data points indicate that the operational limit of torque

was reached at this WOB. A trend line with R^2 = 0.9641 estimated the maximum ROP of approximately 123 ft/hr at 35k-lbs.

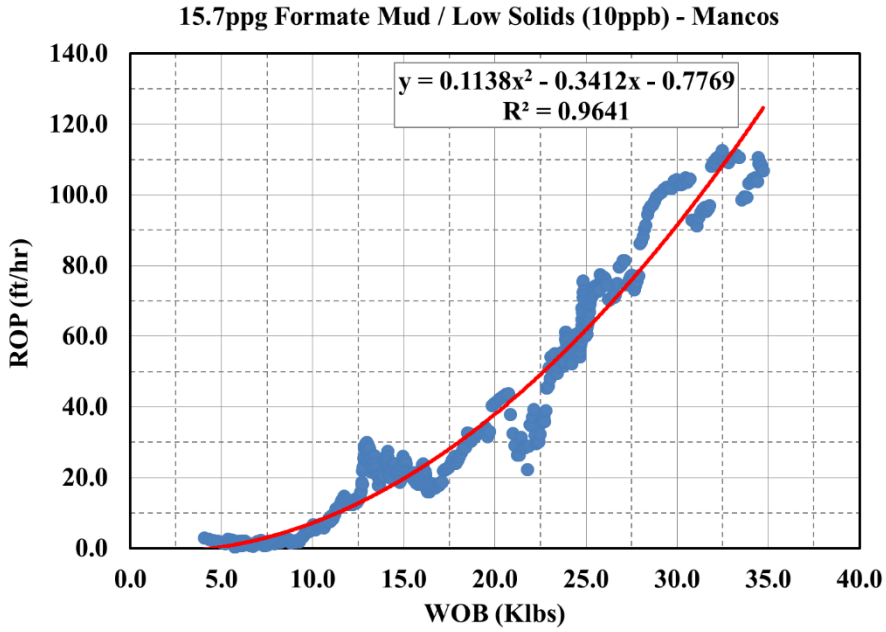

Figure 4.11: ROP vs. WOB data for test 4 – Mancos shale drilled with 15.7ppg formate mud / low solids (10ppb). A regression line with R^2 = 0.9641 is fitted to the data.

4.3.4 Results Cycle 3 – 15.7ppg Formate Mud / High Solids (40ppb)

Once the drilling for cycle 2 was completed, an extra 30ppb of calcium carbonate was added to the used mud and drilling for cycle 3 was carried out. Thus, the drilling mud for this cycle had a water activity of 0.25 and a solids concentration of 40ppb. This was still the concentrated solution of formate blend (15.7ppg) having the PV and YP in the same range as cycle 2 drilling mud.

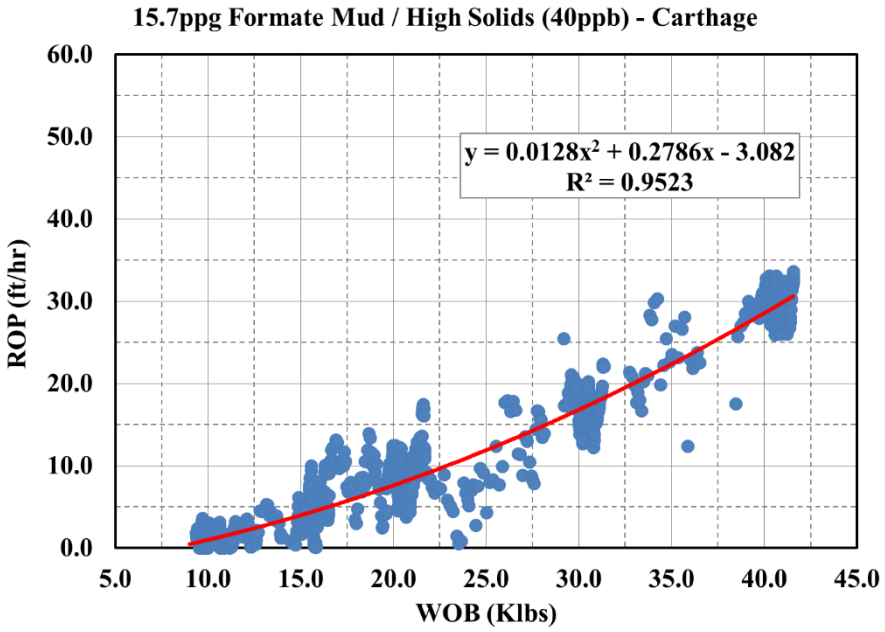

Figure 4.12: ROP vs. WOB data for Test 5 – Carthage limestone drilled with 15.7ppg formate mud / high solids (40ppb). A regression line with R^2 = 0.9523 is fitted to the data.

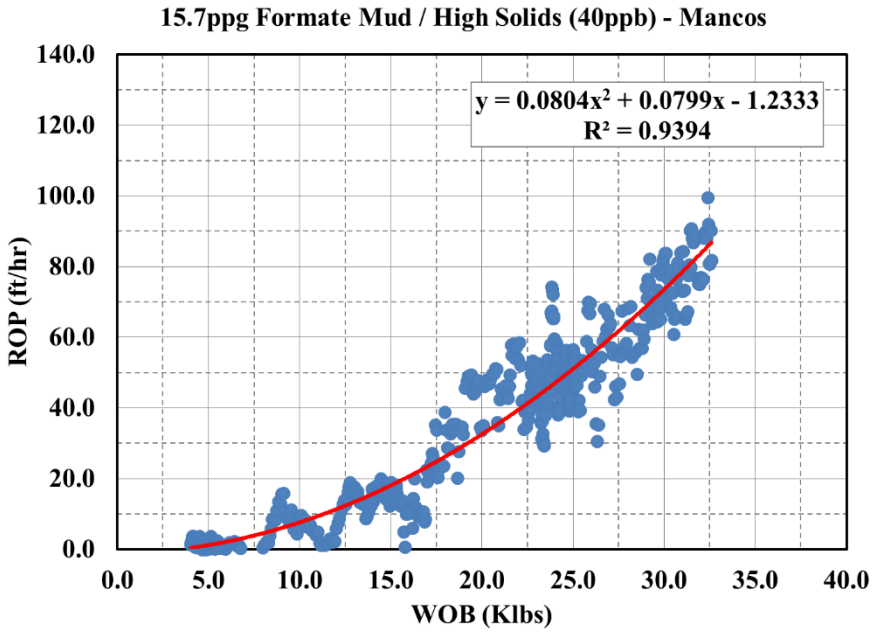

Figure 4.13: ROP vs. WOB data for Test 6 – Mancos shale drilled with 15.7ppg formate mud / high solids (40ppb). A regression line with R^2 = 0.9394 is fitted to the data.

ROP vs. WOB data for test 5 which was carried out in Carthage are represented in Figure 4.12. The data show WOB stops at 10, 15, 20, 30, and 40 k-lbs. and the trend line (R^2 = 0.9523) estimated a maximum ROP of approximately 30ft/hr at 43 k-lbs. Similarly data for test 6 are shown in Figure 4.13. Here, Mancos shale was drilled with cycle 3 mud. WOB stops were predominantly made at 5, 15 and 25 k-lbs. with relatively few data points at higher WOBs. The increase in solids concentration affected ROP, whose maximum value was estimated (from the trend line of R^2 = 0.9394) to be approximately 87ft/hr (this was around 120ft/hr in cycle 2). These comparisons are discussed in detail in the next chapter.

4.3.5 Results Cycle 4 – 11.2ppg Formate Mud / Low Solids (10ppb)

Cycle 4 represents drilling tests carried out in a high water activity (0.825) formate mud with a 10ppb solids concentration. This mud was a diluted solution of the formate blend with a density of 11.2ppg. PV and YP of the mud were in the range of 12 – 13cP and 18 – 19lb/100ft^2, respectively.

Drilling data from test 7 are shown in Figure 4.14. Carthage was drilled with the 11.2ppg mud at WOBs of 10, 20, 30, and 40k-lbs. The trend line having R^2 = 0.9734 was fitted to the curve, which estimated a maximum ROP of 38ft/hr at 40k-lbs. Similarly, Mancos data (test 8) are represented in Figure 4.15. Again due to the torque limitation

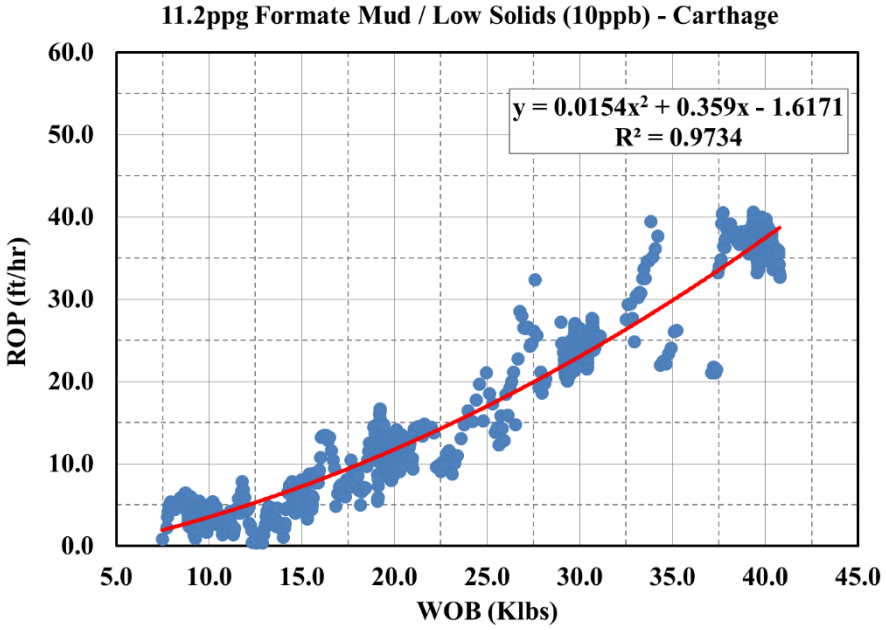

Figure 4.14: ROP vs. WOB data for Test 7 – Carthage limestone drilled with 11.2ppg formate mud / low solids (10ppb). A regression line with R^2 = 0.9734 is fitted to the data.

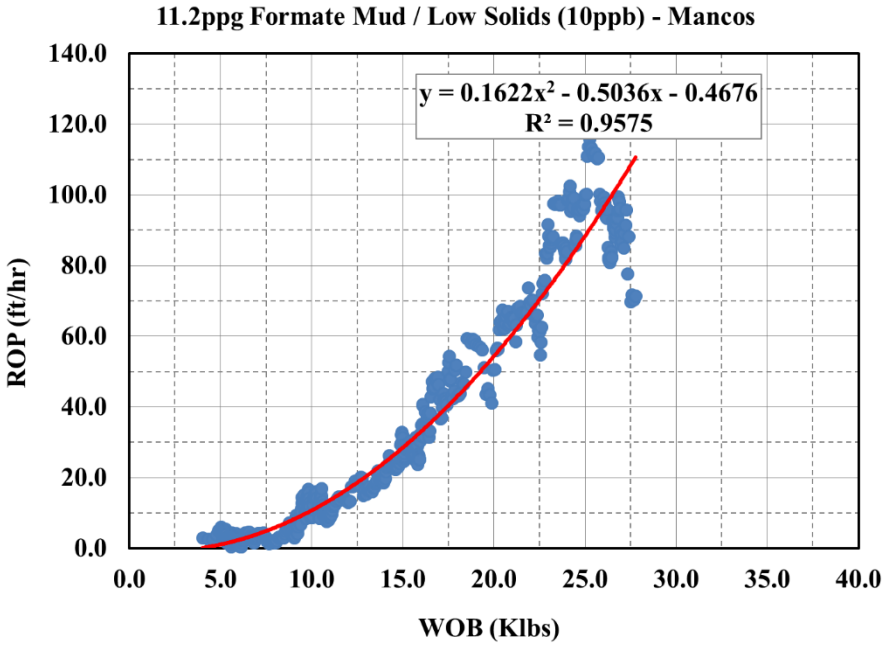

Figure 4.15: ROP vs. WOB data for Test 8 – Mancos shale drilled with 11.2ppg formate mud / low solids (10ppb). A regression line with R^2 = 0.9575 is fitted to the data.

WOB was not increased beyond 25 – 28k-lbs and a maximum ROP of 110ft/hr was estimated from the drawn trend line.

4.3.6 Results Cycle 5 – 11.2ppg Formate Mud / High Solids (40ppb)

Similar to low water activity cycles 2 and 3, once the drilling for cycle 4 was completed, an extra 30ppb of calcium carbonate was added to the used mud and drilling for cycle 5 was carried out. Thus, the drilling mud for this cycle had a water activity of 0.825 and a solids concentration of 40ppb. It was still the diluted solution of formate blend (11.2ppg), having PV and YP in the same range as cycle 4 drilling mud.

Figure 4.16 shows the ROP vs. WOB data for test 9, when cycle 5 mud was used to drill Carthage limestone. The figure clearly shows the WOB stops at 10, 20, 30, and 40k-lbs. A second degree trend line was fitted to the curve, which had a regression coefficient of 0.9524. It estimated a maximum ROP of approximately 34ft/hr at around 40k-lbs WOB.

Similarly, Mancos data from test 10 are represented in Figure 4.17. Again, the maximum WOB achieved was on the order of 27 – 28k-lbs. The trend line whose R^2 = 0.9523 estimated a maximum ROP of approximately 90ft/hr at around 28k-lbs WOB.

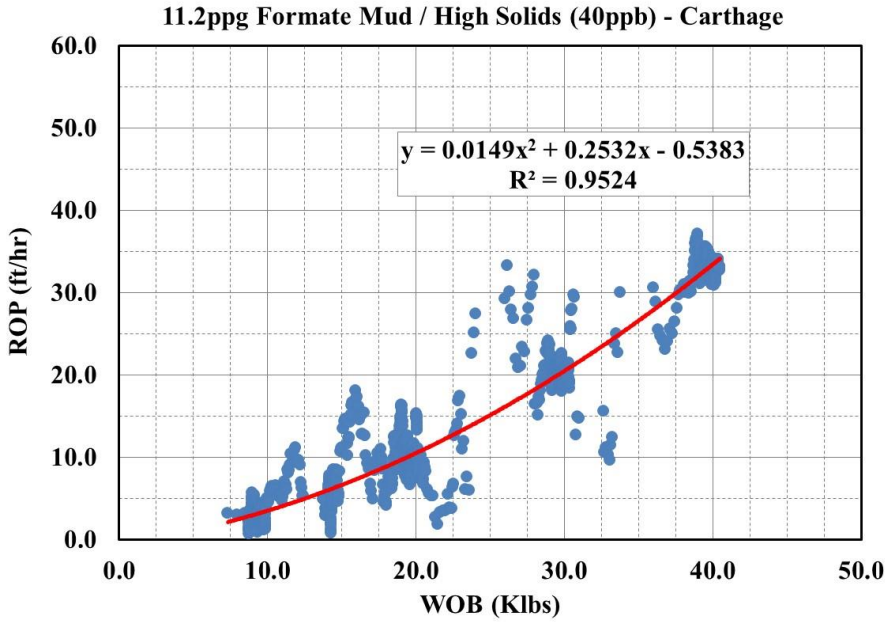

Figure 4.16: ROP vs. WOB data for Test 9 – Carthage limestone drilled with 11.2ppg formate mud / high solids (40ppb). A regression line with $R^2 = 0.9524$ is fitted to the data.

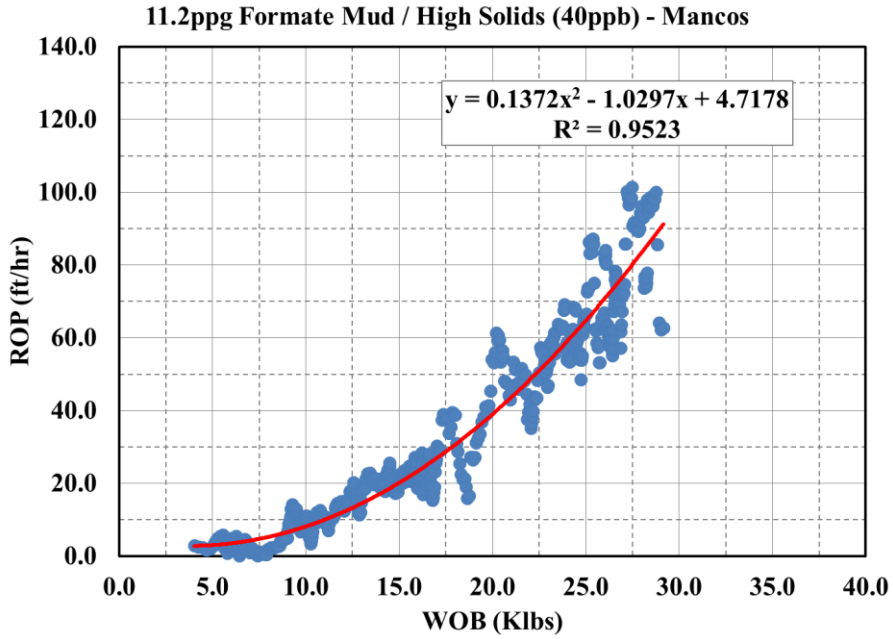

Figure 4.17: ROP vs. WOB data for Test 10 – Mancos shale drilled with 11.2ppg formate mud / high solids (40ppb). A regression line with $R^2 = 0.9523$ is fitted to the data.

4.3.7 Results Cycle 6 – 16ppg Baseline (Kill) Mud

The last cycle of drilling experiments was carried out in high mud weight 16ppg fresh-water WBM. Similar to cycle 1, data obtained from this cycle were also used in comparative analysis with formate mud; however, the 16ppg results were compared with 15.7ppg formate mud (cycles 4 and 5). While the YP of this mud was very high at ~ 64lb/100ft^2, its PV was still around 11cP.

Carthage (test 11) and Mancos (test 12) results are shown in Figures 4.18 and 4.19, respectively.

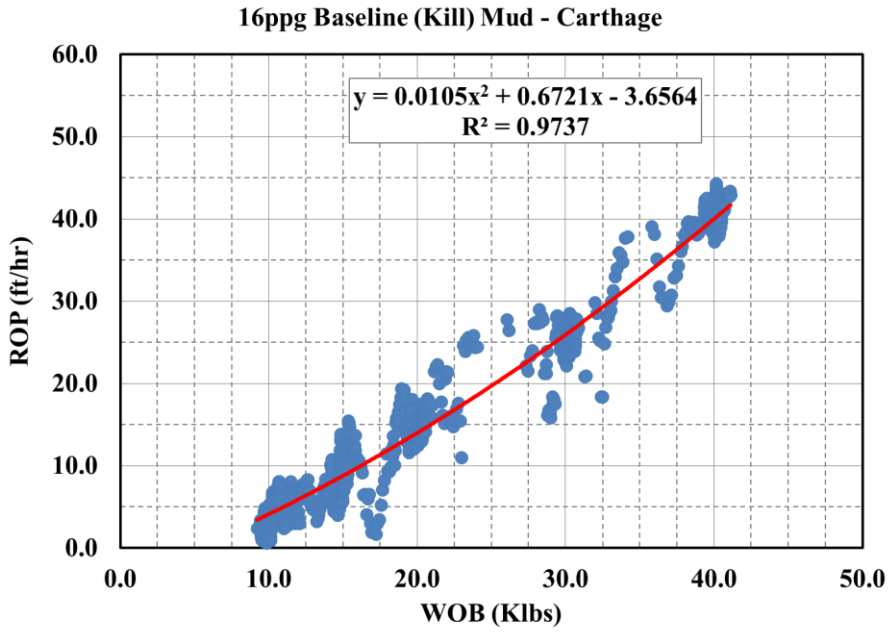

Figure 4.18: ROP vs. WOB data for Test 11 – Carthage limestone drilled with 16ppg baseline (kill) mud. A regression line with $R^2 = 0.9737$ is fitted to the data.

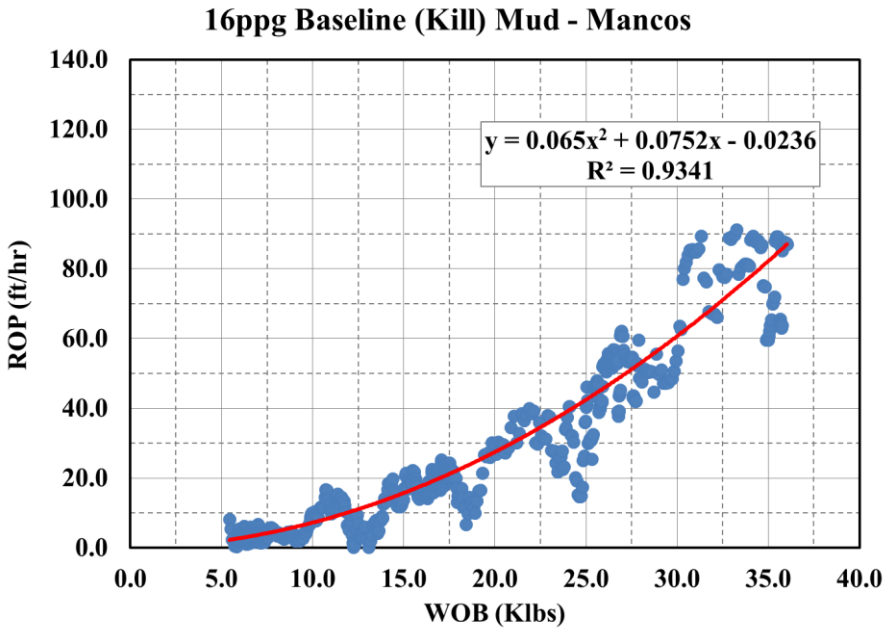

Figure 4.19: ROP vs. WOB data for Test 12 – Mancos shale drilled with 16ppg baseline (kill) mud. A regression line with $R^2 = 0.9341$ is fitted to the data.

Chapter 5: Discussion and Field Results

5.1 INTRODUCTION

The individual results reported in chapter 4 are compiled for a performance comparison among the different drilling fluids. First, the accretion tendencies of different water activity solutions of cesium and potassium formate are compared with the fresh water mud. Next, the WOB vs. ROP curves obtained from drilling simulator tests for different drilling fluids are plotted together; 11.2ppg formate mud is compared with 9.5ppg fresh water mud while 15.7ppg formate mud is compared with 16ppg kill mud. The last section of the chapter discusses positive field trials involving formate mud in Canada.

5.2 DISCUSSION

Both the qualitative and the quantitative results obtained from the accretion experiments prove the 'anti-accretion' tendencies of the formate mud system. As seen from the accretion pictures presented in Chapter 4 and from Figure 5.1, accretion tendencies decrease with lowering water activity (or increasing salinity) which coincides with increasing osmotic pressure.

The presence of solids content in the mud affects the magnitude of shale accretion as an increase in the solids concentration increases the accretion tendencies. This effect of

solids is consistent with Ramsey (1996) and Black et al. (2008) and also coincides with the drilling simulator results presented earlier and discussed later.

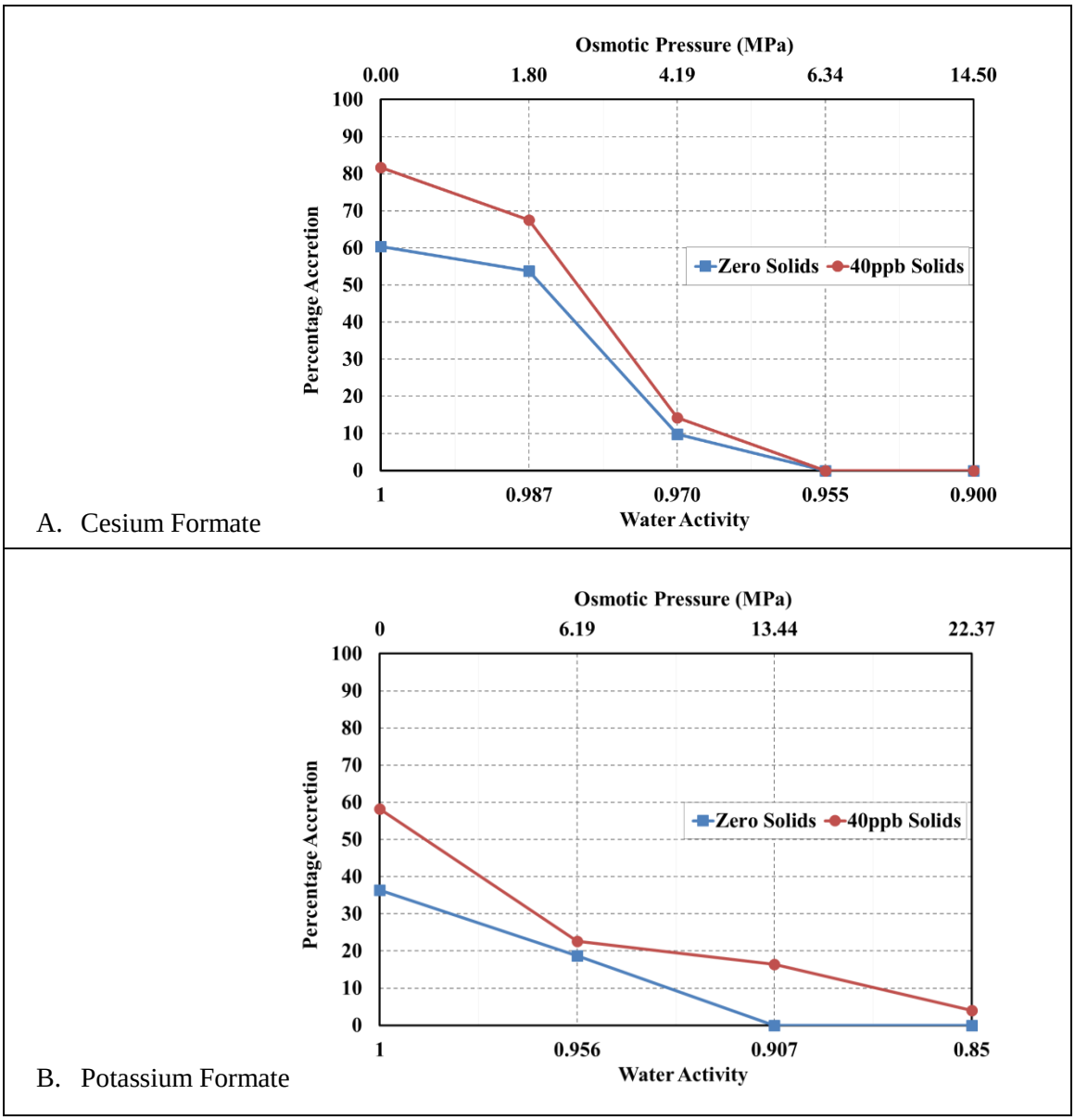

Figure 5.1: Results from accretion experiments on cesium and potassium formate muds for zero and 40ppb solids concentration. Percentage accretion decreases as water activity decreases (or corresponding osmotic pressure increases).

The effect of chemical osmosis is also evident from Figure 5.1, which causes a reduction in accretion as osmotic pressure is increased. In the laboratoty set-up used for the accretion studies, cesium formate completely eliminated accretion at the osmotic pressure of 6.34 MPa regardless of the solids concentration in the mud. However, there were still some accreted solids in potassium formate mud even at 22.37 MPa. This suggests that chemical osmosis is not the only phenomenon that controls the accretion mechanism. This difference in anti-accretion tendency of the two formate mud systems is largely caused by the difference in inhibition capabilities of the two involved cations. Cesium ions are better inhibitors of clay swelling than potassium ions and this apparently translates into cesium formate having slightly better anti-accretion capabilities than potassium formate.

Figure 5.2 and 5.3 show the effect of chemical osmosis while drilling Mancos shale with formate muds in the drilling simulator. The comparison of trend lines obtained for 9.5ppg baseline fresh water (FW) mud and 11.2ppg high water activity formate mud is shown in Figure 5.2. The red solid line in the figure represents the 9.5ppg FW mud. At lower WOBs, all the curves overlap; however, as the WOB increases, the effect of water activity and the osmotic pressure kicks in and the curves begin to diverge. For instance, at 25Klbs, low solids formate mud drills at 88ft/hr , 60% faster than FW mud, which drills at 56ft/hr at the same WOB. However, this improvement is reduced to 15% when the system is loaded up to 40ppb solids. The difference between the two formate curves in the figure explains the effect of solids and corresponds with our earlier observation in small-scale accretion tests.

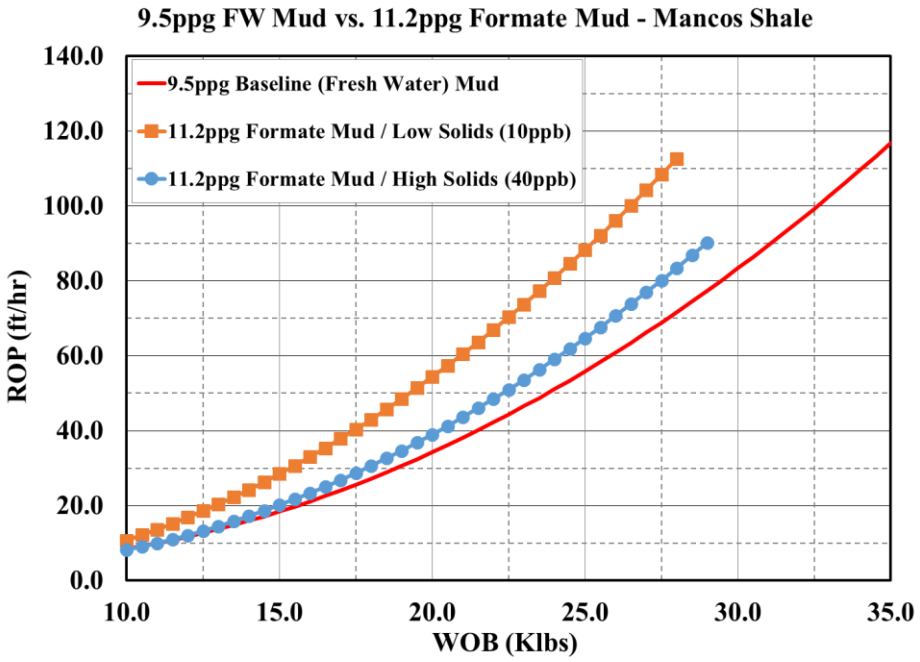

Figure 5.2: Effect of chemical osmosis on Mancos shale in downhole simulator tests. 11.2ppg formate mud, irrespective of the solids concentration, drills faster than the baseline 9.5ppg fresh water mud. However, high solids mud drills slower than the low solids mud.

Figure 5.3 represents the comparison of trend lines obtained for 16ppg baseline kill mud and 15.7ppg low water activity formate mud. Again, there is no difference at lower WOBs and considerable improvement at higher WOBs. At 30Klbs,low solids formate mud drills 50% faster than the base mud (93ft/hr vs. 61ft/hr), while high solids formate mud drills 20% faster.

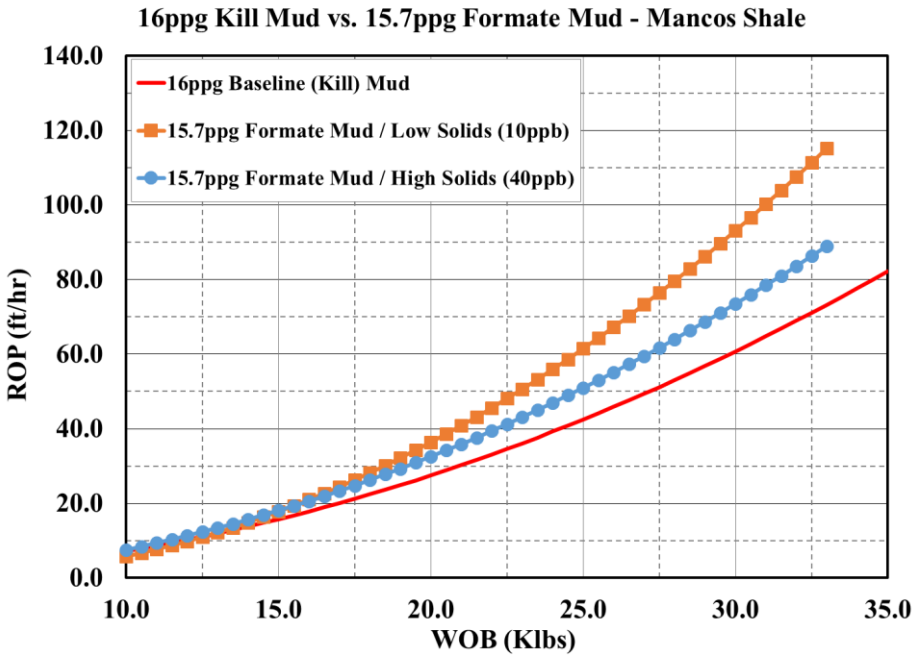

Figure 5.3: Effect of chemical osmosis on Mancos shale in downhole simulator tests. 15.7ppg formate mud, irrespective of the solids concentration, drills faster than the baseline 16ppg fresh water mud. However, high solids mud drills slower than the low solids mud.

The drilling result for Carthage limestone is shown in Figure 5.4. Unlike the shale sample, the Carthage core was not wrapped or preserved. It was a completely dry sample of limestone. Therefore, no effect of water activity or chemical osmosis was expected on the formation. All the curves in Figure 5.4 are bounded within a tight band and appear identical within the experimental error range. Hence, as expected, no clear ROP enhancement effect is seen in this formation.

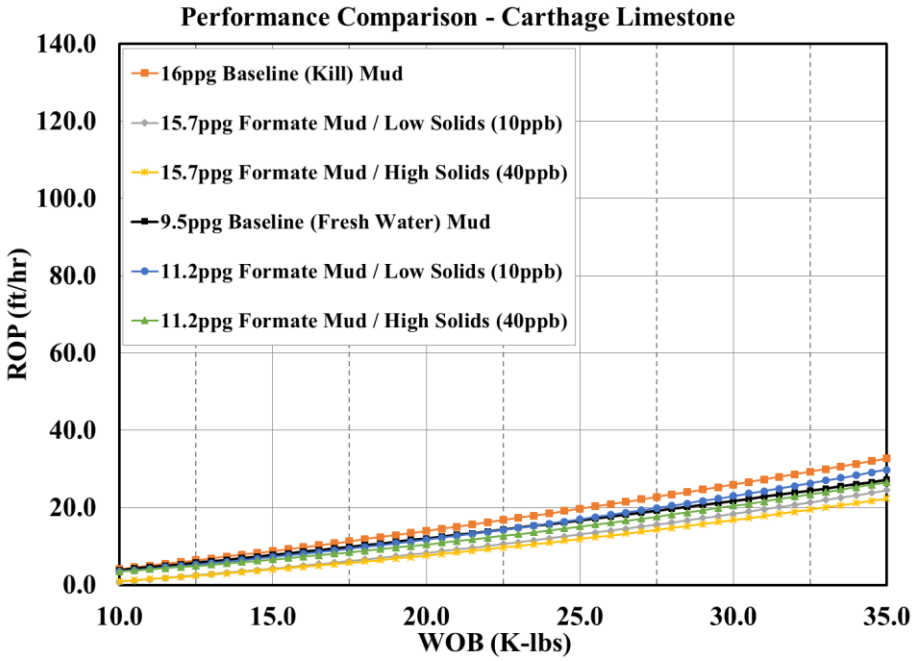

Figure 5.4: No effect of chemical osmosis on Carthage limestone in downhole simulator tests. All the drilling fluids including 9.5ppg and 16ppg fresh water muds, 11.2ppg low and high solids formate mud, and 15.7ppg low and high solids formate mud showed similar performance in drilling tests.

5.3 FIELD TEST RESULTS

The use of formate mud as a drilling fluid dates back to 2001 when two exploration wells (Goliath and Gamma) in Barents Sea, for the first time, were drilled with a mixed sodium/potassium formate system (Offshore Magazine, August 2001). Goliath was drilled 11.8 days ahead of schedule with recorded ROP of around 49 – 82 ft/hr in shale-based formations. Similarly, Gamma was drilled in 5 days less than the expected duration. A penetration rate as high as 107 ft/hr was measured in clay-rich intermediate and reservoir zones. Both of these drilling results correspond to our drilling simulator results achieved

by drilling with mixed cesium/potassium formate brine. The quality of cuttings in both these exploration wells was similar to those generated by oil-based (OBM). The mud system had a good rheological profile and impressive hole cleaning and wellbore stability properties. Since June 2013, more than 120 wells have been drilled with potassium formate in Western Canada. Figure 5.5 (van Oort et al., 2015) represents the performance comparison of formate fluid versus invert mud in drilling a lateral section of 'Montney Field A'.

Montney laterals (siltstone and shale) were typically drilled with a weighted invert system (red lines), which suffered slower ROP and multiple bit runs. However, once this system was replaced with 1.25 – 1.30 SG solids-free potassium formate brine (blue lines), a 30% to 50% increase in ROP was observed and the average bit life was doubled. As a result, the operator has drilled more than 45 laterals with formate mud with a substantial reduction in drilling days, as seen in Figure 5.5. ROP increase was not observed in drilling upper Montney sands, which is consistent with the benefits of formate fluids being primarily achieved in shales.

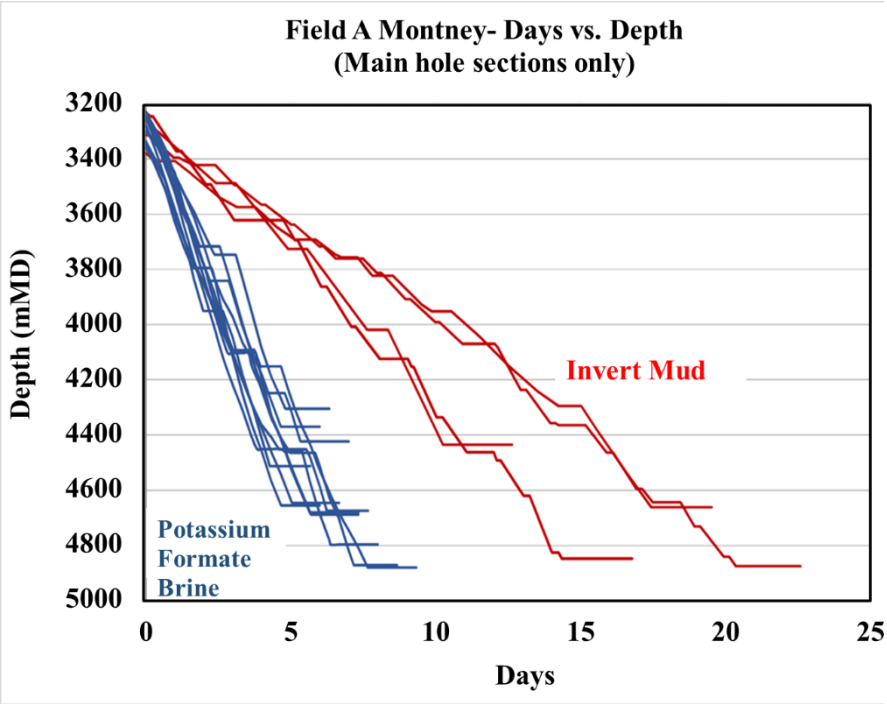

Figure 5.5: Potassium formate mud drilling performance compared to invert mud in Montney Field A (van Oort et al., 2015). A substantial reduction in drilling days can be seen when invert mud is switched with formate mud in main hole sections only.

Figure 5.6 (van Oort et al., 2015) shows the performance comparison of formate fluid versus invert mud in 'Montney Field B Trial Well # 1'. Once the mud system was switched to formate mud, the ROP nearly doubled and the average bit life tripled. For a direct comparison between the two mud systems, the first formate well was displaced to OBM for the last 86m of the horizontal and ROP was instantly reduced by half. WOB was increased but it proved impossible to match the ROP achieved with the formate system.

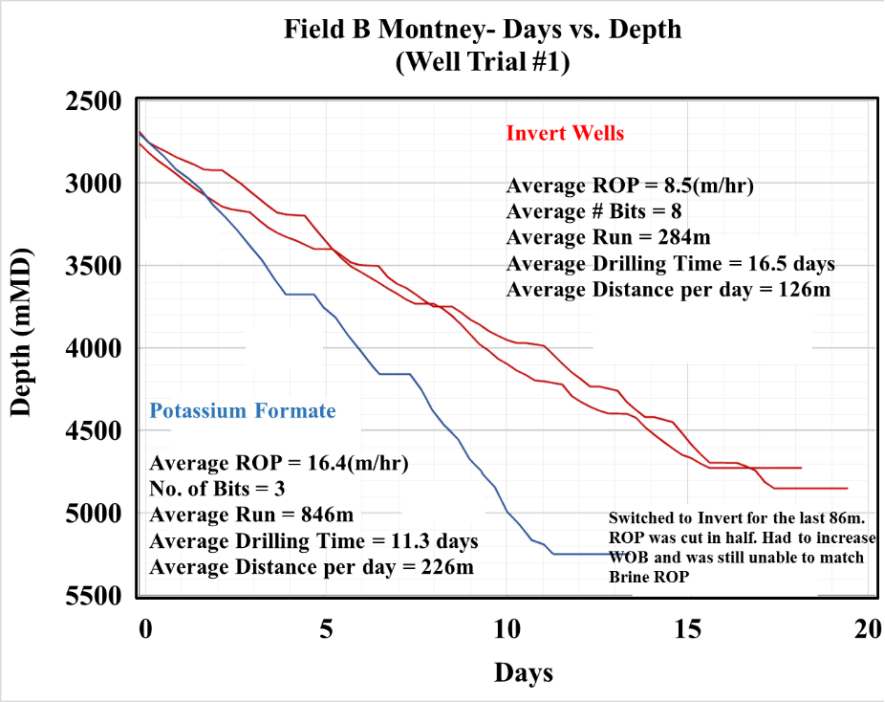

Figure 5.6: Potassium formate mud drilling performance compared to invert mud in Montney Field B Trial well #1 (van Oort et al., 2015). ROP doubles and bit life triples when invert mud is switched with formate mud.

Trial well # 2, shown in Figure 5.7 was also a successful well, drilled with potassium formate mud. The well was drilled with 2 bit runs only versus 8 bit runs in the invert mud. Similarly, the average ROP was also 80% higher in the formate system.

Seeing the advantages of formate mud in drilling lateral sections in the Montney fields, the benefits were then explored in the intermediate well sections. Presently, wells are drilled with surface casing using Floc-water and intermediate and main hole sections with formate mud. Figure 5.8 (van Oort et al., 2015) estimates a reduction of 10 – 15 days on average when OBM is replaced with formate mud.

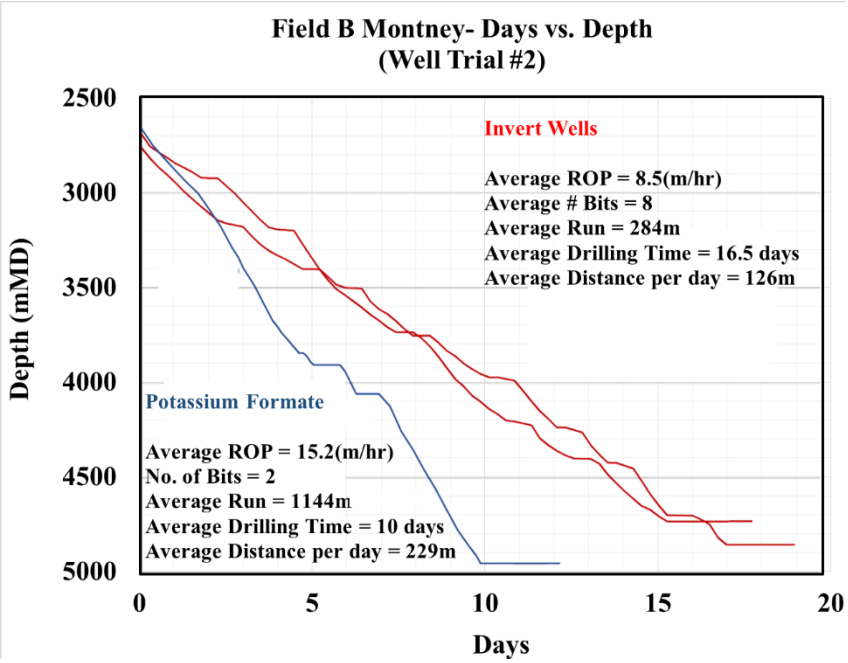

Figure 5.7: Potassium formate mud drilling performance compared to invert mud in Montney Field B Trial well #2 (van Oort et al., 2015). Reduction in drilling days and increase in ROP can be seen when invert mud is switched with formate mud.

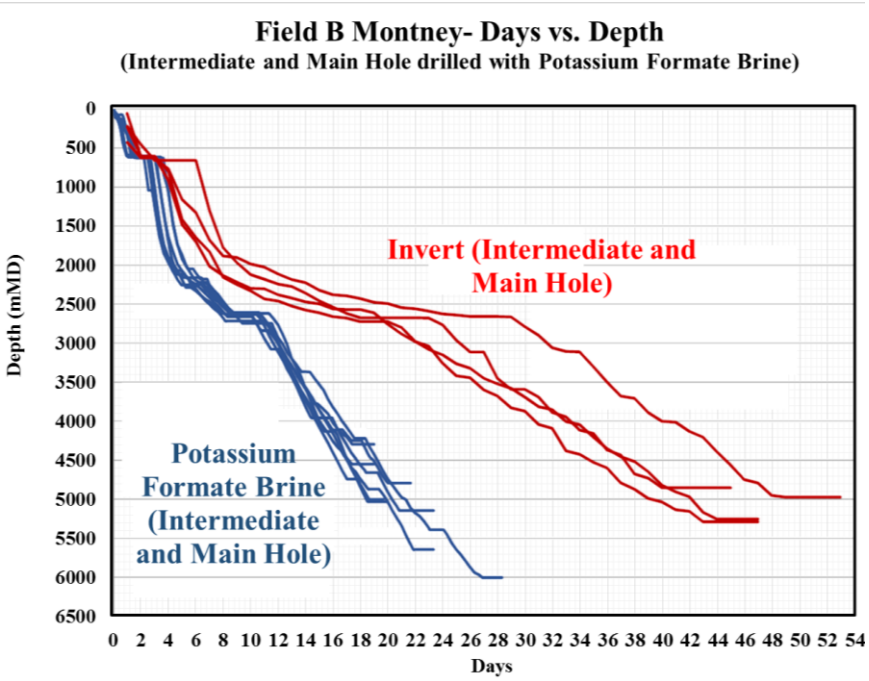

Figure 5.8: Potassium formate mud drilling performance compared to invert mud in Montney Field B (van Oort et al., 2015). 50% reduction in drilling time can be seen when invert mud is switched with formate mud in intermediate and main hole sections.

Chapter 6: Conclusions and Recommendations

6.1 CONCLUSIONS

The ROP enhancement results obtained from the drilling simulator experiments and from the Canadian field trials appear to be consistent with the proposed mechanism of chemical osmosis. The high-salinity formate muds generate osmotic pressures high enough to draw water out of shale. This water forms a thin lubricating layer over the surface of the bit and reduces the sticking tendency of clay. It then allows the cutter to be cleaned more effectively with the available horse power, yielding a substantial increase in rates of penetration. Drawing the water molecules out of shale also strengthens the outer layer of the shale, which behaves less plastically than a fully hydrated shale layer and thus is less prone to sticking and balling.

One can argue that the benefits observed in the experiments are due to clay inhibition (i.e., suppression of hydration of clay minerals in the shales). However, note that OBM/SBM are the best inhibitive muds and provide the ultimate inhibitive action by not allowing the hydration of shales; formate mud out-drilled the OBM in both the Deep Trek experiments and the Canadian field trials. Moreover, such ROP enhancement effects have not been seen in KCl / polymer muds, which also provide excellent inhibition qualities; the reason is the high water activities and low osmotic pressures in KCl / polymer muds. The analogy of chemical osmosis to electro-osmosis, whose effects were established in Literature Review section of the thesis, also supports the fact that the ROP enhancement

effects in the Deep Trek experiments, drilling simulator tests, and Canadian field trials were all likely to be caused by chemical osmosis.

From the set of experiments performed during the research and from the study of Canadian field trials, the following points can be put forward:

Cesium and potassium formate have excellent anti-accretion tendencies. Fresh water mud corresponding to a solution of water activity 1.00 showed maximum accretion (60% – 80%) among all the studied fluids. Adding formate content to the mud (i.e., decreasing water activity of the solution or increasing the associated osmotic pressure) significantly reduces the accretion tendency of the corresponding mud. For instance, a 16% by volume solution of cesium formate reduces water activity of the drilling mud from 1.00 to 0.955 and generates an osmotic pressure of 6.34Mpa, high enough to reduce accretion to zero.

Together with the water activity and osmotic pressure, the inhibition capabilities of the studied formate systems also play a vital role in limiting the accretion tendencies of the drilling mud. Cesium and potassium ions both, effectively suppress the processes of hydration and the swelling of clays, prevent further dispersion of cuttings, and help to decrease accretion. Cesium ions are better inhibitors of clay swelling than potassium ions; thus, cesium formate is slightly better than potassium formate in controlling accretion. While it took a 16% by volume solution of cesium formate (osmotic pressure = 6.34MPa) to completely eliminate accretion in our laboratory setup, potassium formate required a 24% by volume solution with an associated osmotic pressure of 22.37 MPa to do the task.

The presence of solids interferes with the inhibitive capabilities of formate mud and consequently exacerbates accretion. The higher the solid content in the drilling mud, the higher the accretion tendency of the mud and the higher the formate content required to act against accretion. Thus, it is recommended to keep the drilling fluids as clean as possible.

Downhole simulator drilling tests in Mancos shale showed a 50% – 60% increase in ROP when fresh water mud is replaced with the corresponding weight formate mud (e.g., 9.5ppg FW mud replaced by 11.2ppg formate mud, 16ppg kill mud replaced by 15.7ppg formate mud). This improvement in ROP grows further as the WOB increases. Thus, all other factors being constant, a substantial increase in ROP can be achieved at higher drilling depths corresponding to higher WOBs. However, due to the dry nature of rock samples, there was zero to no effect of formate mud in Carthage limestone as all the drilling fluid recorded more or less similar drilling data within an expected error range.

As seen in the accretion experiments, the presence of solids in the drilling mud affects the formate mud performance. The ROP benefits, which in the presence of 10ppb solids is at 50% – 60%, reduce to 15% – 20% when the system is loaded up to 40ppb solids. This reduction in ROP improvement can be attributed to the accumulation of colloidal solids at the interface between the cutter and the shale formation and thus interference with obtaining benefits from the water layers.

Drilling results from the Canadian field trials coincide with our findings and on average show a 50% reduction in drilling time when the invert mud is switched with potassium formate mud. These results also prove that formate brines tend to maximize bit

life. This could be due to the fact that higher ROP in formate mud means fewer revolutions at a particular RPM, which results in less wear. Furthermore, lubrication of the cutters with the water layer minimizes friction and keeps the cutters cool. All these factors enhance the life of a bit, which can be translated to reduction in drilling time and cost.

6.2 RECOMMENDATIONS FOR FUTURE WORK

Initially, three sets of experiments to support our proposed hypothesis were planned:

1. Small-scale Accretion Experiments
2. Medium-scale Micro-bit Rig Experiments
3. Large-scale Drilling Simulator Experiments

However, due to logistics constraints and considerable hardware issues, we could not perform the micro-bit tests. The micro-bit rig installed at Baker Hughes is a small-scale drilling rig that drills 3.875” x 3.750” core samples through its 1 1/8” PDC bit. Drilling fluids for these tests (i.e., 13.10ppg potassium formate and 18.30ppg cesium formate) were provided by Cabot. Since the micro-bit rig requires a small volume of drilling fluid (18-20gallons) to run a test, it is possible to study a wide range of water activity solutions. Thus, completing this set of testing is recommended to strengthen belief in the proven hypothesis. Tables 6.1 and 6.2 show the recommended mud compositions /preparation and test matrix for the micro-bit experiments.

Table 6.1: Recommended mud composition / preparation for micro-bit rig experiments (to prepare 25gal drilling mud)

Base Fluid	Density (ppg)	Water Activity	Potassium Formate (gal)	Cesium Formate (gal)	Water (gal)	XC Polymer (lbs.)
Fluid 01	13.10	0.26	25.00	0.00	0.00	0.75
Fluid 02	18.30	0.30	0.00	25.00	0.00	0.75
Fluid 03	16.30	0.29	9.90	15.10	0.00	0.75
Fluid 04	14.10	0.50	7.14	10.88	7.16	0.75
Fluid 05	12.20	0.70	4.73	7.20	13.36	0.90
Fluid 06	9.80	0.90	1.77	2.70	20.87	1.10

Table 6.2: Recommended test matrix for micro-bit rig experiments. Tests No. 1, 2, 15, and 16 are the baseline tests in water- and oil-based muds. The rest of the tests are formate mud tests for different water activity formate solutions as defined in Table 6.1.

Test No.	Fluid Type	Fluid Name / Density	Solids Content	Rock
1A	Fresh Water	9.5 ppg	-	Carthage
1B				Mancos
2A		16 ppg	-	Carthage
2B				Mancos
3A	Formate Fluids	Fluid 01	10 ppb	Carthage
3B				Mancos
4A			40 ppb	Carthage
4B				Mancos
5A		Fluid 02	10 ppb	Carthage
5B				Mancos
6A			40 ppb	Carthage
6B				Mancos

Table 6.2(continued): Recommended test matrix for micro-bit rig experiments.

Test No.	Fluid Type	Fluid Name / Density	Solids Content	Rock
7A	Formate Fluids	Fluid 03	10 ppb	Carthage
7B				Mancos
8A			40 ppb	Carthage
8B				Mancos
9A		Fluid 04	10 ppb	Carthage
9B				Mancos
10A			40 ppb	Carthage
10B				Mancos
11A		Fluid 05	10 ppb	Carthage
11B				Mancos
12A			40 ppb	Carthage
12B				Mancos
13A		Fluid 06	10 ppb	Carthage
13B				Mancos
14A			40 ppb	Carthage
14B				Mancos
15A	Oil-based Mud	10 ppg	-	Carthage
15B				Mancos
16A		16 ppg	-	Carthage
16B				Mancos

Following are other recommendations for future work to further investigate the osmotic processes for ROP enhancement:

1. The results of this study proved the formate benefits in shale, which were further confirmed by the Canadian field results. A separate investigation should be carried out to study the effects of such high-salinity muds in other formations.
2. To fully validate the proposed osmotic mechanism, it would be useful to study other high-salinity, low water activity muds that also can generate osmotic movement of water molecules.
3. Electro-osmosis has been studied on the laboratory scale and has established potential benefits. Further study should therefore be directed toward large-scale experiments by drilling under realistic downhole conditions.

Acronyms

ABC	:	Anti-balling coating
bbl	:	Barrel
$CaCl_2$	:	Calcium chloride
cp	:	Centi poise
Cs	:	Cesium
CsFo	:	Cesium Formate
ECD	:	Equivalent circulating density
EIA	:	Energy information administration
EPA	:	Environmental Protection agency
FV	:	Face volume
FW	:	Fresh water
gal	:	Gallon
HCOO-	:	Formate ion
HPHT	:	High pressure high temperature
HSI	:	Hydraulic horsepower per square inch
in	:	Inch
JSA	:	Junk slot area
K	:	Potassium
KCl	:	Potassium Chloride
ksi	:	Kilo pounds per square inch
lbs.	:	Pounds
MD	:	Measured depth
Mn	:	Manganese
MPa	:	Mega Pascal
MSE	:	Minimum specific energy

µm	:	Micro meter
Na	:	Sodium
nm	:	Nano meter
OBM	:	Oil-based mud
PDC	:	Poly-crystalline diamond compact
PHPA	:	Partially hydrolyzed poly-acrylamide
ppb	:	Pounds per barrel
ppg	:	Pounds per gallon
psi	:	Pounds per square inch
PV	:	Plastic viscosity
ROP	:	Rate of penetration
RPM	:	Revolutions per minute
SBM	:	Synthetic-based mud
SPP	:	Solid particular phase
WBM	:	Water-based mud
WOB	:	Weight on bit
YP	:	Yield point

Nomenclature

a_w	:	Water activity (frac)
a_w^{df}	:	Water activity of drilling mud (frac)
a_w^{shale}	:	Water activity of shale (frac)
D	:	Diffusivity of water in clay (m^2/sec)
$d\varphi/dt$	:	Rate of change of concentration (mol/m^3sec)
$d\varphi/dx$	:	Concentration gradient (mol/m^4)
M_i	:	Water content of unexposed bentonite tablets (frac)
P_{mud}	:	Mud pressure (psi)
P_{pore}	:	Pore pressure (psi)
$P_{swelling}$	:	Swelling pressure of clay (psi)
R	:	General gas constant (J/mol.K)
R^2	:	Regression Coefficient (frac)
T	:	Temperature (K)
$\bar{V}_w$	:	Molar volume of water (m^3/mol)
V_{stock}	:	Volume of stock brine (lab bbl)
V_{water}	:	Volume of water (lab bbl)
W_1	:	Weight of the cuttings added to the jar (gm)
W_2	:	Weight of the wet cuttings scrapped off the bar (gm)
W_3	:	Weight of the dried cuttings (gm)
x	:	Displacement of water front (m)
$\%wt_{req}$	:	Required weight percentage of formate in base brine (%)
$\%wt_{stock}$	:	Weight percentage of formate in stock brine (%)

σ	:	Membrane efficiency (%)
$\sigma^{eff}{}_r$	:	Radial effective stress (psi)
ρ_{req}	:	Required density of base brine (ppg)
ρ_{stock}	:	Density of stock brine (ppg)
$\varphi(x,t)$	:	Concentration as a function of length and time (mol/m^3)
φ_0	:	Original concentration (mol/m^3)
ΔP	:	Hydraulic overbalance of drilling mud (psi)
$\Delta\Pi_{osmotic}$	:	Osmotic pressure (psi)
$\Delta\Pi^{eff}_{osmotic}$	:	Effective osmotic pressure (psi)

References

Al-Bagoury, M., and Steele, C. (2014), Potassium formate / Manganese Tetraoxide Fluid for Ultra HPHT Drilling. American Association of Drilling Engineers. Paper AADE-14-FTCE-44

Anbah, S. A., Chilingar, G. V., and Beeson, C. M. (1965). Application of electrokinetic phenomena in civil engineering and petroleum engineering. Annals of the New York Academy of Sciences, 118(14), 587-602.

Black, A. D., Bland, R. G., Curry, D., Ledgerwood, L. W., Robertson, H., Judzis, A., and Grant, T. (2008). Optimization of Deep-Drilling Performance with Improvements in Drill-Bit and Drilling-Fluid Design. Society of Petroleum Engineers. doi: 10.2118/112731-MS

Bland, R., Jones, T., & Tibbitts, G. A. (1997, January 1). Reducing Drilling Costs by Drilling Faster. Society of Petroleum Engineers. doi: 10.2118/38616-MS

Chenevert, M. E. (1970). Shale Control with Balanced-Activity Oil-Continuous Muds. Society of Petroleum Engineers. doi: 10.2118/2559-PA

Clark, R. K., Scheuerman, R. F., Rath, H., and Van Laar, H. G. (1976). Polyacrylamide/Potassium-Chloride Mud for Drilling Water-Sensitive Shales. Society of Petroleum Engineers. doi: 10.2118/5514-PA

Cooper, G. A., and Roy, S. (1994). Prevention of Bit Balling by Electro-Osmosis, Society of Petroleum Engineers. doi: 10.2118/27882-MS

Darley, H., and Gray, G. (1988). Composition and properties of drilling and completion fluids (5th ed.). Houston, TX: Gulf Pub., Book Division

Davis, E. H., and Poulos, H, G. (1980). The relief of negative skin friction on piles by electro-osmosis. University of Sydney, Research report R-367

De Stefano, G., and Young, S. (2009). The Prevention And Cure Of Bit Balling In Water Based Drilling Fluids. Offshore Mediterranean Conference. 2009-110 OMC Conference Paper

Downs, J. D. (2006). Drilling and Completing Difficult HPHT Wells with the Aid of Cesium Formate Brines – A Performance Review. Society of Petroleum Engineers. doi:10.2118/24973-MS

Downs, J. D. (1993). Formate Brines: Novel Drilling and Completion Fluids for Demanding Environments. Society of Petroleum Engineers. doi: 10.2118/25177-MS

Downs, J. D., Killie, S., and Whale, G. F. (1994). Development of Environmentally Benign formate-Based Drilling and Completion Fluids. Society of Petroleum Engineers. doi:10.2118/27143-MS

Downs, J. D., Howard, S. K., and Carnegie, A. W. (2005). Improving Hydrocarbon Production Rates Through the Use of Formate Fluids – A Review. Society of Petroleum Engineers. doi:10.2118/97694-MS

Downs, J. D. (2006). Drilling and Completing Difficult HPHT Wells with the Aid of Cesium Formate Brines – A Performance Review. Society of Petroleum Engineers. doi:10.2118/99068-MS

Downs, J. D. (2010). A Review of the Impact of the Use of Formate Brines on the Economics of Deep Gas Field Development Projects. Society of Petroleum Engineers. doi:10.2118/130376-MS

Dupriest, F. E., and Koederitz, W. L. (2005). Maximizing Drill Rates with Real-Time Surveillance of Mechanical Specific Energy. Society of Petroleum Engineers. doi:10.2118/92194-MS

Eggestad, A., and Foyn, T. (1983). Electro-osmotic improvement of a soft sensitive clay. Proceedings of the 8th ECSMFE, 2, 597-603.

Esrig, M. I. (1978). Increasing Offshore Pile Drivability through Electroosmosis. Offshore Technology Conference. doi: 10.4043/3269-MS

Fear, M. J., Meany, N. C., and Evans, J. M. (1994). An Expert System for Drill Bit Selection. Society of Petroleum Engineers. doi:10.2118/27470-MS

Gilbert, Y. M., Wemyss, P., Gaches, P., Smith, D. (2003). Formate Brines Environmental Assessment. Metoc plc, Report no. 1147

Gilbert, Y. M., Pessala, P., Vaahtera, A., and Raivio, T. (2007). Formate Fluids and Environmental Regulations: A Global View of Benefits and Challenges. Society of Petroleum Engineers. doi:10.2118/110891-MS

Garcia-Gavito, D., and Azar, J. J. (1994). Proper Nozzle Location, Bit Profile, and Cutter Arrangement Affect PDC-Bit Performance Significantly. Society of Petroleum Engineers. doi:10.2118/20415-PA

Glowka, D. (1983). Optimization of Bit Hydraulic Configurations. Society of Petroleum Engineers. doi:10.2118/10240-PA

Hale, A. H. (1991). Method to Quantify Viscosity Effects on Dispersion Test Improves Testing of Drilling-Fluid Polymers. Society of Petroleum Engineers, doi:10.2118/19954-PA

Hale, A. H., Mody, F. K., and Salisbury, D. P. (1993). The Influence of Chemical Potential on Wellbore Stability. Society of Petroleum Engineers. doi:10.2118/23885-PA

Hariharan, P. R., Cooper, G. A., and Hale, A. H. (1998). Bit Balling Reduction by Electro-Osmosis While Drilling Shale Using a Model BHA (Bottom Hole Assembly). Society of Petroleum Engineers. doi:10.2118/39311-MS

Helmholtz, H. (1879). Studien über elektrische Grenzschichten. Wiedemanns Annalen d. Physick, 7, 137

Holster, J. L., and Kipp, R. J. (1984). Effect of Bit Hydraulic Horsepower on the Drilling Rate of a Polycrystalline Diamond Compact Bit. Society of Petroleum Engineers. doi: 10.2118/11949-PA

Howard, S., Formate Technical Manual. Retrieved from http://www.cabotcorp.com/solutions/products-plus/cesium-formate-brines/technical-manual

Iwata, S., Tabuchi, T., and Warkentin, B. (1988). Soil-Water Interactions: Mechanisms and Applications (1st ed.). Marcek Dekker

Judzis, A., Black, A. D., Curry, D. A., Meiners, M. J., Grant, T., and Bland, R. G. (2007). Optimization of Deep Drilling Performance; Benchmark Testing Drives ROP Improvements for Bits and Drilling Fluids, Society of Petroleum Engineers. doi:10.2118/105885-MS

Kooi, H., Garavito, A., and Bader, S. (2003). Numerical modelling of chemical osmosis and ultrafiltrationacross clay formations. Journal of Geochemical Exploration, 78-79, 333-336

Ledgerwood, L. W. and Kelly, J. L. Jr. (1991). High Pressure Facility Recreates Downhole Condition in Testing of Full Sized Drill Bits. American Society of Mechanical Engineers. Paper ASME 91-PET-1

Ledgerwood, L. W. (2007), PFC Modeling of Rock Cutting Under High Pressure Conditions, American Rock Mechanics Association, Paper ARMA-07-063

Low, P. (1961). Physical Chemistry of Clay Water Interaction. Advances in Agronomy, 13, 269-327.

Martin, R. (1960). Adsorbed Water on Clay: A Review. Clays and Clay Minerals. Proceedings of the Ninth National Conference on Clays and Clay Minerals, 9, 28-70.

Mitchell, J., and Soga, K. (2005). Fundamentals of soil behavior (3rd ed.). Hoboken, N.J.: John Wiley and Sons.

Offshore Magazine (2001). Drilling Technology: Na/K Formate Brine Using as Drilling Fluid in Sensitive Barents Sea Wells

Pessier, R. C., and Fear, M. J. (1992). Quantifying Common Drilling Problems With Mechanical Specific Energy and a Bit-Specific Coefficient of Sliding Friction. Society of Petroleum Engineers. doi:10.2118/24584-MS

Probstein, R. F., and Hicks, R. E. (1993). Removal of contaminants from soils by electric fields. Science, 260(5107), 498-503.

Ramsey, M. S., Shipp, J. A., Lang, B. J., Black, A., and Curry, D. (1996). Cesium Formate: Results and Analysis of Drilling with a New High Density Unweighted Brine. Society of Petroleum Engineers. doi:10.2118/36425-MS

Remmert, S. M., Witt, J. W., and Dupriest, F. E. (2007). Implementation of ROP Management Process in Qatar North Field. Society of Petroleum Engineers. doi:10.2118/105521-MS

Rose, W. L., and Grubbs, B. R. (1979). Field Applications of Electro Osmosis to Increase Offshore Pile Driveability. Offshore Technology Conference. doi:10.4043/3444-MS

Roy, S., and Cooper, G. A. (1991), Effect of Electro-Osmosis on the Indentation of Clays, American Rock Mechanics Association. Paper ARMA 91-335

Sánchez, F. G., Loon, L. R., Gimmi, T., Jakob, A., Glaus, M. A., Diamond, L. W. (2008), Self-Diffusion of Water and Its Dependence on Temperature and Ionic Strength in Highly Compacted Montmorrilonite, Illite and Kaolinite. Applied Geochemistry, 23(12), 3840-3851.

Schmid, G. (1950). Zur Elektrochemie feinporiger Kapillarsysteme. In Angewandte Chemie . 62(16), 387-387)

Siemens, R, and Meyer, E. (2014). Using Formate Brine and Water Based Drilling Fluids to Improve Drilling Performance – A Case Study in Pipestone, Encana Corporation Presentation. Retrieved from: http://www.slideshare.net /manfromgwelo/shale-drilling-with-potassium-formate-brine-chevron-encana-presentation

Smith, L., Mody, F. K., Hale, A., and Romslo, N. (1996). Successful Field Application of an Electro-Negative Coating to Reduce Bit Balling Tendencies in Water Based Mud. Society of Petroleum Engineers. doi:10.2118/35110-MS

Smith, R. H., Lund, J. B., Anderson, M., & Baxter, R. (1995). Drilling Plastic Formations Using Highly Polished PDC Cutters. Society of Petroleum Engineers. doi:10.2118/30476-MS

Smoluchowski (1914) in Graetz, L. (1918). Handbuch der Elektrizität und des Magnetismus (Vol. 2). Leipzig: J.A. Barth.

Speer, J. W. (1959). A Method for Determining Optimum Drilling Techniques. Society of Petroleum Engineers. doi:10.2118/1242-G

Spiegler, K. (1958). Transport processes in ionic membranes. Transactions of the Faraday Society, 54, 1408-1428.

Titkov, N. I. (1961). Electrochemical Induration of Weak Rocks. Translated by Consultants Bureau, New York.

U.S. Energy Information Administration. (2013). Technically Recoverable Shale Oil and Shale Gas Resources: An Assessment of 137 Shale Formations in 41 Countries outside

the United States. Retrieved from: http://www.eia.gov/analysis/studies /worldshalegas/pdf/overview.pdf

U.S. Energy Information Administration. (2014). Annual Energy Outlook 2014 with Projections to 2040. Retrieved from: http://www.eia.gov/forecasts/aeo/. DOE/EIA-0383(2014)

van Oort, E., Ahmad, M., Spencer, R., and Legacy, N. (2015). ROP Enhancement in Shales through Osmotic Processes. Society of Petroleum Engineers. doi:10.2118/173138-MS

van Oort, E., Bland, R., & Pessier, R. (2000). Drilling More Stable Wells Faster and Cheaper with PDC Bits and Water Based Muds. Society of Petroleum Engineers. doi:10.2118/59192-MS

van Oort, E., Hale, A. H., and Mody, F. K. (1995). Manipulation of Coupled Osmotic Flows for Stabilisation of Shales Exposed to Water-Based Drilling Fluids. Society of Petroleum Engineers. doi:10.2118/30499-MS

van Oort, E., Hale, A. H., Mody, F. K., and Roy, S. (1996). Transport in Shales and the Design of Improved Water-Based Shale Drilling Fluids. Society of Petroleum Engineers. doi:10.2118/28309-PA

van Oort, E. (1997). Physico-Chemical Stabilization of Shales. Society of Petroleum Engineers. doi:10.2118/37263-MS

van Oort, E. (2003). On the physical and chemical stability of shales. Journal of Petroleum Science and Engineering, 38(3-4), 213-235

Warren, T. M., and Armagost, W. K. (1988). Laboratory Drilling Performance of PDC Bits. Society of Petroleum Engineers. doi:10.2118/15617-PA

Wells, M., Marvel, T., and Beuershausen, C. (2008). Bit Balling Mitigation in PDC Bit Design. Society of Petroleum Engineers. doi:10.2118/114673-MS

Wrixon, R. C., and Cooper, G. A. (1998). Theoretical and Practical Application Guidelines for Using Electrokinetics to Improve Casing Support in Soft Marine Sediments. Society of Petroleum Engineers. doi:10.2118/39299-MS

Zijsling, D. H., and Illerhaus, R. (1993). Eggbeater PDC Drillbit Design Eliminates Balling in Water-Based Drilling Fluids. Society of Petroleum Engineers. doi:10.2118/21933-PA

Zuvo, M., Bjornbom, E., Ellingsen, B., Downs, J. C., Kelley, A., and Trannum, H. C. (2005). High-Resolution Environmental Survey Around an Exploration Well Drilled

With Formate Brine in the Barents Sea, Norway. Society of Petroleum Engineers. doi:10.2118/94477-MS